F I N A L R E P O R T

European Space Agency
European Space Operations Centre (ESOC)

Contract No. 5443/83/D/IM(SC)

STUDY ON THE USE AND CHARACTERISTICS OF SAR FOR GEOLOGICAL APPLICATIONS

PART II: RADARGRAMMETRY ASPECTS

G. DOMIK, E. KIENEGGER, F. LEBERL, J. RAGGAM

Institute for Image Processing and Computer Graphics
Graz Research Center
Wastiangasse 6
A-8010 Graz, Austria

Graz, June 1985

ABSTRACT

Radargrammetric processing of radar images is required as a preparatory step in a multitude of subsequent applications, and as an application field in its own right. The existing radargrammetric literature and past theoretical analyses of radargrammetric problems are thoroughly reviewed and examined. The influence of specific imaging and flight parameters relevant in the field of geological applications, such as the elevation angle and the flight direction, is investigated using radar imagery from past experiments and to a much greater extend by using simulated data. A geological interesting test area (Sardegna, Italy) was chosen to suggest processing algorithms for the creation of radar ortho images as a step to merge radar images to other data sets (e.g. data from geological maps) and subsequent non-linear feature extraction. A method to create a digital elevation model from radar stereo images is presented. The influence of elevation angle and flight direction on the data quantity and quality is investigated and proved by using the advantages of a simulator.

1 INTRODUCTION

One of the important systems for satellite remote sensing is side-looking imaging radar. First experiences were gained in the Apollo 17 Lunar Sounder (ALSE) experiment (Phillips et al., 1973). An attempt at a global terrestrial radar mapping system was made with SEASAT (Teleki und Ramseier, 1978), creating an enormous data set that has inspired a great number of studies, in spite of the experiment's early failure after a mere 3 months in space.

Other spaceborne radar imagery is available only from the Shuttle Imaging Radar A (SIR-A) from a short orbital flight (Ford, Cimino, Elachi, 1983).

As a result of these missions today there exist four satellite radar data sets for use in scientific work. Additional imagery is scheduled to become available in a series of additional flights of the Space Shuttle, and from European, Canadian and Japanese experiments.

One may well state that the scope of data for applications studies is rather limited when considering satellite systems. This is different from the situation with aircraft-side-looking radar. Since the early 1960's ongoing aircraft activities have led to a coverage of entire countries.

As a result, SLR image maps at scale of about 1:250,000 were generated for countries such as, for example, Brazil (de Azevedo, 1971), Venezuela (McKeon, 1979), Panama (Crandall, 1969), Guatemala, Nigeria and Togo (Dellwig, 1980), and for portions of other countries such as Indonesia (Froidevaux, 1980), the Philippines, Colombia (Leberl, 1974), Peru (Martin-Kaye, 1980), the U.S.A. and others. SLR clearly was the most "operational" new remote sensing device (apart from photography) until the advent of Landsat remote sensing (Mathews, 1975).

Currently, a trend can be observed in the U.S. with NASA and other agencies (Radar Geology, 1980), in Europe with ESA and its co-operative research projects, and in Japan, to apply SLR-work not only in exploration, but also to vegetation, inundation, sea-ice and others. A noticeable slant towards radar studies is evident in recent IEEE-conferences on "Geoscience and Remote Sensing", the latest in S. Francisco (IGARSS, 1983).

The reason for this interest may well be the independence from weather: after all, even Landsat-type imaging with an interval of 18 and 16 days respectively between repeated coverages of a given area did not, in many areas of the world, provide sufficient useful images for monitoring-tasks and multi-temporal studies. Of a given area in Austria, to give just one example, there is no cloud-free Landsat image at all during the year 1980.

The increased thoroughness of SLR research has led to a need for better image geometry, so that radar images can be compared to other data and to images taken at different

times. While early radar maps were compiled with little attention to geometric accuracy, there is now an interest emerging in techniques of radar photogrammetry, or "radargrammetry", a term coined by Levine (1960), then still in the context of the plan position indicator.

The radargrammetry aspects of SLR have greater importance in satellite projects than in imaging from aircraft because small neglections of these aspects already have great consequences on geometric accuracy. To give but one example, a satellite`s velocity is roughly 40-times higher than an aircraft's. Consequently those functions of the velocity that reasonably can be neglected when considering aircraft radar may not be negligible for a satellite.

The first part of this report (section 1 to 4) presents a review of radargrammetric literature, an evaluation of past experiments and of current theoretical understanding. The second part covers the definition of specific parameters relevant for radargrammetric applications. A test area, chosen by the requirements of availability of radar data, existence of geological information (geological maps) and geological interest in this area, is presented and described by the existing data of radar imagery and geological and topographic maps. Processing algorithms for radar imagery (including a radar image simulator, radar rectification, the generation of a digital elevation model and extraction of distributed surface features) are described in theory and practical applications. The results of these applications lead to predictions and conclusion for future radar satellite missions.

Author of section 1 to 4 is F. L e b e r l . Chapter 7.4 on radar stereo-mapping was elaborated by J . R a g g a m . All other parts were prepared by G . D o m i k with assistance of E. K i e n e g g e r (image processing aspects).

After the final presentation of the project some changes and improvements to the draft were made by M. B u c h r o i t h n e r , mainly in the chapters 6, 7.4 and 8.2 to 8.4.

2 REVIEW OF RADARGRAMMETRIC LITERATURE

Earliest radargrammetric references relate to the circularly scanning plan position indicator (PPI), a radar system that was of some interest to Earth mapping during the 1950's (Rinner, 1948; Macchia, 1957). It is of no relevance today in remote sensing. One can classify the published references in several categories. They will be addressed in the following.

2.1 Basic Mathematical Formulation

2.1.1 Literature

Radargrammetry requires a mathematical model relating an object point in some three-dimensional cartesian X, Y, Z coordinate system to the time and range coordinates, t and r, measurable from the side-looking radar record. Such models were presented and discussed by numerous authors, among them Konecny and Derenyi (1966), Akowetzki (1968), Derenyi (1970), Rosenfield (1968), Gracie et al. (1970), Leberl (1970), Hockeborn (1971), and Norvelle (1972). In all cases radargrammetry begins with the SLR-image, not with the raw electronic signals acquired by the antenna.

However, a trend in digital radar systems is developing to go beyond the radar record and to look into raw, unprocessed signals. First indications are visible in studies by Kratky (1979), Brown et al. (1981), and Curlander (1981 a, b). These new approaches rely on concepts such as "sensor events time", i.e. the exact time when a raw pulse was transmitted from and received by the radar antenna, and how the raw radar echo is converted into image points.

Numerous authors have formulated rigorous radar projection equations, similar to the so-called rigorous photogrammetric equations for photography. The intent of these formulations is to model the typical range projection. Object points are projected along concentric circles onto a projection plane. Authors who have contributed here are Rinner (1948), Konecny and Derenyi (1966), Rosenfield (1968), Akowetzki (1968), Derenyi (1970), Gracie et al. (1970), Leberl (1970),Hockeborn (1971), Geier (1972), Greve and Cooney (1974), DBA-Systems (1974) and many authors since. A review was compiled by Leberl (1976b).

2.1.2 Equations

It is necessary to define in a radar image an image point P by its sensor event time t, and slant range between antenna and object, r_s, possibly based on coordinate measurements x_k, y_k in some rectangular measurement system (Figure 1).

Generally we may therefore just define an operator F:

$$r = F_r(x_k, y_k)$$
$$t = F_t(x_k, y_k) \qquad (1)$$

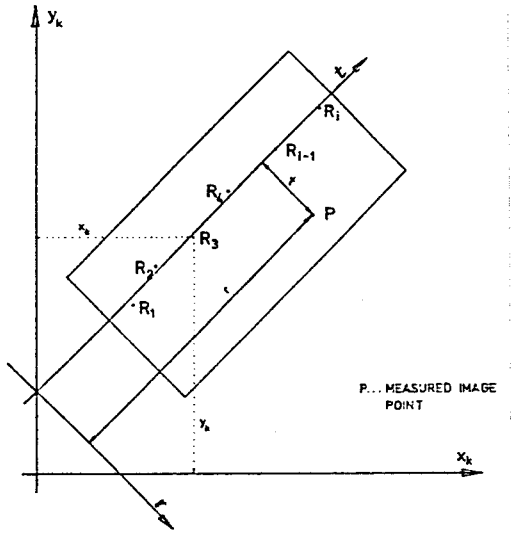

FIGURE 1: Measuring coordinates in a side-looking radar; x_k, y_k are comparator coordinates, r, t, are range and time coordinates.

In certain types of radar images, particularly those designed for good geometry, one may find auxiliary reference marks, such as those of Figure 1, denoted by R_1, R_2 etc. Depending on the type of marks we can define the form of Equ. (1) and its parameters.

Proper radargrammetric equations define the sensor position, $\underline{s}(t)$, and antenna attitude, $\phi(t)$, $\omega(t)$, $\kappa(t)$. In synthetic aperture radar, the synthetic antenna's attitude is merely the first derivative of position, namely the velocity vector $\dot{\underline{s}}(t) = (\dot{s}_x(t), \dot{s}_y(t), \dot{s}_z(t))$. Both $\underline{s}(t)$ and $\dot{\underline{s}}(t)$ are functions of time t. The formulation also requires a definition of object and sensor coordinate systems according to Figure 2, with unit vectors, $\underline{e}_1$, $\underline{e}_2$, $\underline{e}_3$ and $\underline{u}$, $\underline{v}$, $\underline{w}$, respectively.

We then find for an object point P its position vector $\underline{p}$:

$$\underline{p} = p_x\underline{e}_1 + p_y\underline{e}_2 + p_z\underline{e}_3 \qquad (2)$$

and in the sensor system

$$\underline{r} = u_p\underline{u} + v_p\underline{v} + w_p\underline{w} \qquad (3)$$

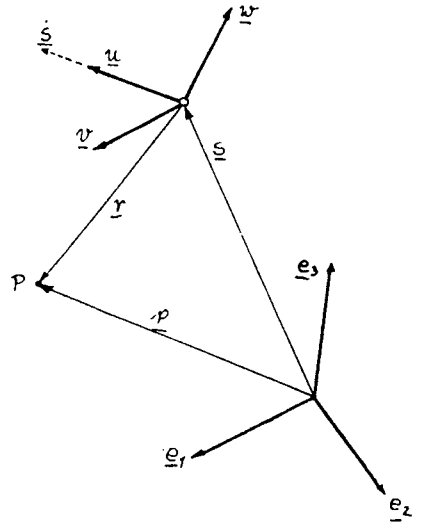

FIGURE 2: Definition of object space and sensor coordinate systems.

Therefore,

$$\underline{p} = \underline{s} + \underline{r} \qquad (4)$$

It is straightforward to see from Figure 3 that

$$\begin{aligned} u_p &= r\cdot\sin\tau \\ v_p &= r\cdot(\sin^2\Omega - \sin^2\tau)^{1/2} \\ w_p &= -\,r\cdot\cos\Omega \end{aligned} \qquad (5)$$

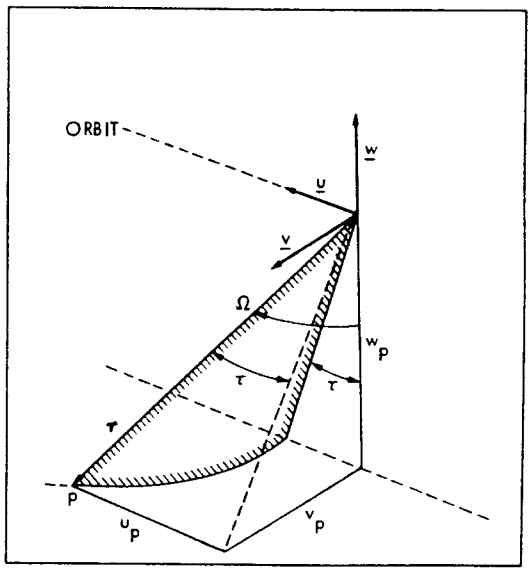

FIGURE 3: Relating squint angle τ, slant range r and elevation angle Ω to sensor coordinates u,v,w.

The auxiliary angle τ is a system constant called squint-angle by most authors (Rosenfield, 1968; Hockeborn, 1971) and defines the conical shape of the radar beam.

Introducing a new vector $\bar{p} = (u_p, v_p, w_p)$ in the sensor coordinate system and a rotation matrix $\underline{A}$ to rotate the sensor system u, v, w into the object system $\underline{e}_1$, $\underline{e}_2$, $\underline{e}_3$, we find in matrix notation:

$$\underline{p} = \underline{s} + \underline{A} \cdot \bar{p} \tag{6}$$

where

$$\underline{A} = \begin{bmatrix} u_x(t) & u_y(t) & u_z(t) \\ v_x(t) & v_y(t) & v_z(t) \\ w_x(t) & w_y(t) & w_z(t) \end{bmatrix} \tag{7}$$

Rotation matrix $\underline{A}$ can contain the classical orientation angles ϕ, ω and κ if we deal with a real antenna. With synthetic antennas, we obtain:

$$\begin{aligned} \underline{u} &= (u_x, u_y, u_z) = \dot{\underline{s}}/|\dot{\underline{s}}| \\ \underline{v} &= (v_x, v_y, v_z) = (\underline{s} \times \dot{\underline{s}})/|\underline{s} \times \dot{\underline{s}}| \\ \underline{w} &= (w_x, w_y, w_z) = (\underline{u} \times \underline{v})/|\underline{u} \times \underline{v}| \end{aligned} \tag{8}$$

The unit vector $\underline{u}$ extends along the synthetic antenna, thus in the direction of the velocity vector $\dot{\underline{s}}$. The unit vector $\underline{v}$ should be normal to $\underline{u}$ and to the nadir direction of the antenna. For satellite sensors, the nadir direction is easily seen to be the direction of the sensor position vector in a planetocentric system.

With aircraft radar, one has to specify here explicitly that a geocentric system is assumed also for the sensor position vector $\underline{s}$ and the object coordinate system defined by $\underline{e}_1$, $\underline{e}_2$, $\underline{e}_3$.

Equations (5) and (6) relate object and image, where r and time t derive from the image coordinates. We now see that - contrary to classical photogrammetry - we do not algebraically relate image and object coordinates, but the image only defines time, which in turn defines the parameters $\underline{s}$ and $\underline{A}$ of Eq. (6).

If the imaging arrangement, and thus $\underline{s}(t)$, $\underline{A}(t)$, are known (measurement of navigation data), then we have for each point 3 equations (Eq. 6) with 4 unknowns, i.e. Ω, p_x, p_y and p_z. It may be preferable to work with 2 equations and 3 unknowns. This is achieved by eliniation of the unknown elevation angle Ω (angle between nadir and line of sight), thus giving the following two equations:

$$|\underline{p} - \underline{s}| = r \qquad (9)$$

$$\underline{u} \cdot (\underline{p} - \underline{s}) = \sin\tau \, |\underline{u}| \cdot |\underline{p} - \underline{s}| = \sin\tau \cdot r \qquad (10)$$

where we now have a simple geometric description of the radar projection case. The geometric locus of a point is the intersection of range-sphere (Eq. 9) with a cone (Eq. 10). This is the circular projection line mentioned before.

2.1.3 Discussion

The existing body of radargrammetric definitions for the projection equations relate to analog aircraft radar. Discussions concentrate on the satellite radar. So far little has appeared on satellite radargrammetry although more work needs to be done due to the expected future significance of orbital imaging radars. Essential additions in this area are definitions of satellite radar imaging equations not merely as a function of sensor position and attitude, but as a function of orbital parameters such as orbit inclination i, radius a and eccentricity e of the orbit, the angle of the line of apsides, time t and rotation velocity ω of the Earth.

This may serve for image simulations and general radargrammetric analysis. Its discussion goes beyond the scope of this paper. Some work in this area has been done by Manning and Hann (1967) and by Leberl (1978a).

2.2 The Use Of Single Radar Images

2.2.1 General

Work with SLAR-images involves positioning efforts. This requires that details on the image are located in a geographic reference system. Single radar images are the basic unit of data for this procedure. Geographic "referencing" may result in the following:

a) computation of ground coordinates from given image coordinates;

b) generation of a grid overlay over a given image;

c) production of a rectified image, a so-called "ortho-image", using as an input a raw, distorted image and information on the object.

One may differentiate between various cases for the application of radargrammetry to single images; these are described in the following items.

2.2.2 Computation Of Object Coordinates On An Ellipsoid, If The Interior And Exterior Orientation Of The Satellite Sensor Are Known -

This is the typical case of defining an object position on the ocean surface from satellite radar images. An algorithm is iterative and was presented by Leberl (1978a) and by Brown et al. (1981).

2.2.3 Spherical And Plane Objects

The problem described in chapter 2.2.2 simplifies if an image of a spherical or plane object needs to be used. No particular discussion is required: non-iterative algorithms are feasible, of interest and were described by Leberl (1978a).

2.2.4 Computation Of Object Coordinates In The Event Of Unknown Satellite Attitude And Position

An unknown exterior orientation leads to the necessity of using control points or - more generally - control information to relate image and object space. This has been attempted by many authors. The efforts can be classified into:

(a) interpolative models employing so-called "rubber-sheeting" or warping algorithms to make the image fit to ground control;

(b) parametric models employing projection equations and computing unknown parameters from control point information; and

(c) hybrid combination of (a) and (b), where the projection equations are used to relate image and object, but where an interpolative technique is applied to represent unknown deviations of reality from the assumed model.

(a) Polynomials

Various authors have evaluated different types of polynomials for radar image correction (Leberl, 1970; Derenyi, 1974a; Hirsch and van Kuilenburg, 1976; Shakine and LeToan, 1978). A common conclusion is difficult to draw, since different data from different sensors were employed. However, one may summarize that the use of polynomials is generally not advisable due to their predictably unfavourable behavior in the case of irregular control point distribution, and in the case of extrapolation. Polynomials are only recommended if they are of low order (1st or second) and if there is an even control point distribution.

(b) Parametric Models

The exterior orientation of the sensor can be modelled by various mathematical concepts. The rigorous radar projection equations need to be linearized so that an error of the elements of sensor attitude and position is related to the error of the computed object coordinates.

Authors have in the past proposed various mathematical models for the exterior orientation as a function of time, e.g. DBA Systems (1974) employed polynomials.

The analysis of this approach is beyond the scope of this paper. It may, however, be relevant to point out that instead of single high order polynomials it is preferable to use piecewise polynomials of low order. Baker and Mikhail (1974) have studied these approaches, however, for aircraft scanner imagery, not for radar.

Dowideit (1977) studied the method of modelling the exterior orientation parameters by Fourier series, correctly arguing that the elements of the exterior orientation have a periodical behavior with several dominating frequencies (Leberl, 1972a). Again, one has to solve for the unknown coefficients of the Fourier series. The main problem is instability of the resulting equation system due to correlation among coefficients.

A somewhat different approach has been proposed for dynamic scanner images by Ebner and Hoessler (1978). The elements of exterior orientation are considered to form time-series appropriately modelled by Gauss-Markoff-chains of order m.

2.2.5 Computation Of The Image Coordinates Of A Known Object Point And With A Known Satellite Position And Attitude

This problem needs to be solved when the image position of an object needs to be predicted, e.g. in simulation and in geometric correction of images. A solution was described by Leberl and Fuchs (1978) and by Leberl, Fuchs and Ford (1981).

2.2.6 Radar Image Rectification

Actual radar image rectification was done by Leberl and Fuchs (1978) and by Leberl, Fuchs and Ford (1981).

The study by Leberl and Fuchs (1978) presented a detailed error analysis. Its discussion here would go beyond the scope of this paper.

Digital rectification has been done so far in the context of the SEASAT-mission. Curlander et al. (1981) have used digital SAR-images from SEASAT together with orbital data, and Naraghi et al. (1981) matched the SAR-data with a digital terrain model.

There exists the concept of geo-coded imagery (Guertin and Shaw, 1981). This is synonymous with "ortho-images".

Recently image rectification with DHM's has been implemented in a digital image processing environment using simulated images as a reference. The real image is made to fit a simulation based on topographic terrain heights (Domik, Kobrick and Leberl, 1984).

2.2.7 Radar Image Mono-Plotting

Instead of actually creating a geometrically corrected radar image one can think of converting only certain interpreted image details to map projection.

This concept was realized by Greve and Cooney (1974) with radar, and is a method of photogrammetry which has also been proposed by other authors.

However, the idea has not yet had responses of any significance, either with metric photography nor with radar or other image types.

2.3 The Use Of Overlapping Stereo-Imagery

2.3.1 General

Stereo viewing of overlapping images is a valuable tool in photointerpretation. It is also an indispensable technique to identify homologue image points for measurement of image coordinates and reconstruction of a three-dimensional model. This may serve to create a model of terrain topography, such as in the form of contours, or to selectively measure slopes and relative height differences.

For the observer radar stereo is not different from its photographic equivalent. However, there applies an entirely different mathematical model.

Most of the commonly discussed radar stereo-arrangements are denoted by same-side and opposite-side stereo. La Prade (1963) was the first to propose stereo for side-looking radar. Numerous other authors addressed the topic of stereo, however mainly its computational aspects. Stereo viewability was studied by La Prade (1970), Graham (1975, 1976), Leberl (1978a, 1979). Computational aspects were treated by Innes (1964), Rosenfield (1968), Gracie et al. (1970), Konecny (1972), DBA-Systems (1974), Goodyear (1974), Derenyi (1975) and Leberl (1972, 1975c, 1978a).

Apart from the above mentioned stereo cases there have been proposals for cross-wise and other overlapping images from two flight lines (Leberl, 1972b; Graham, 1975). For real aperture radar also single flight convergent schemes

have been discussed by Leberl (1972b), Carlson (1973) and Bair and Carlson (1974, 1975). Single flight stereo cannot be obtained with synthetic aperture radar due to the fact that the projection line of a point is always a circle in a plane perpendicular to the flight line (velocity vector).

2.3.2 Viewability

The two partners of a stereo image pair must be very similar in image quality or thematic content (tone, texture, etc.) so that they correlate well, whereas they should be sufficiently different in geometry to present parallaxes for height perception.

Radar is actively illuminating the object. Differences in geometry due to different sensor positions therefore imply also illumination differences. Good stereo from a geometric point of view therefore contradicts good viewability.

La Prade (1975) reports on one experiment with operators studying same-side stereo of flat areas with man-made objects. Optimum results were reported to require look angles of 37 degrees to 67 degrees off-nadir, and intersection angles of about 12 degrees to 15 degrees.

Lately several authors have begun to simulate images in order to obtain predictions on radar image viewability. Work has been carried out by Kaupp et al. (1982), Leberl, Raggam and Kobrick (1985) and Domik, Leberl and Raggam (1983).

2.3.3 Stereo-Computations

The authors Rosenfield (1968), Gracie et al. (1970), Konecny (1972), DBA Systems (1974) and Leberl (1976) discussed similar approaches to stereo computation based on rigorous formulas.

A general formulation for radar stereo computations is based on Eq. (6), but for two overlapping images denoted by (') and ("):

$$\underline{p} = \underline{s}' + \underline{r}'$$
$$\underline{p} = \underline{s}'' + \underline{r}'' \qquad (11)$$

With the assumption of known interior orientation (conversion of image x, y-coordinates to time t and range r) as well as exterior orientation (sensor position $\underline{s}$, attitude or velocity vector $\dot{\underline{s}}$), expression (9) represents 6 scalar equations with 5 unknowns p_x, p_y, p_z, Ω' and Ω''. We can eliminate $\underline{p}$ from (9) to obtain a co-planarity equation:

$$\underline{s}' + \underline{r}' - \underline{s}'' - \underline{r}'' = 0 \qquad (12)$$

which consists of 3 scalar equations with unknowns Ω' and Ω''. An alternative is to estimate r', r":

$$|\underline{p} - \underline{s}'| = r'$$

$$|\underline{p} - \underline{s}''| = r''$$

$$\dot{\underline{s}}' \cdot (\underline{p} - \underline{s}') = \sin\Omega' \cdot |\dot{\underline{s}}'| \cdot r'$$

$$\dot{\underline{s}}'' \cdot (\underline{p} - \underline{s}'') = \sin\Omega'' \cdot |\dot{\underline{s}}''| \cdot r'' \qquad (13)$$

These are 4 non-linear equations with the three unknowns p_x, p_y and p_z. A solution is through linearisation and iteration.

A simple formulation is based on parallaxes:

The absolute parallax is measured when the flight lines of two images are superimposed. Parallax differences are differences of absolute parallaxes between a given reference and a new point. We need to relate the object height above a reference datum to parallaxes measured in an image pair.

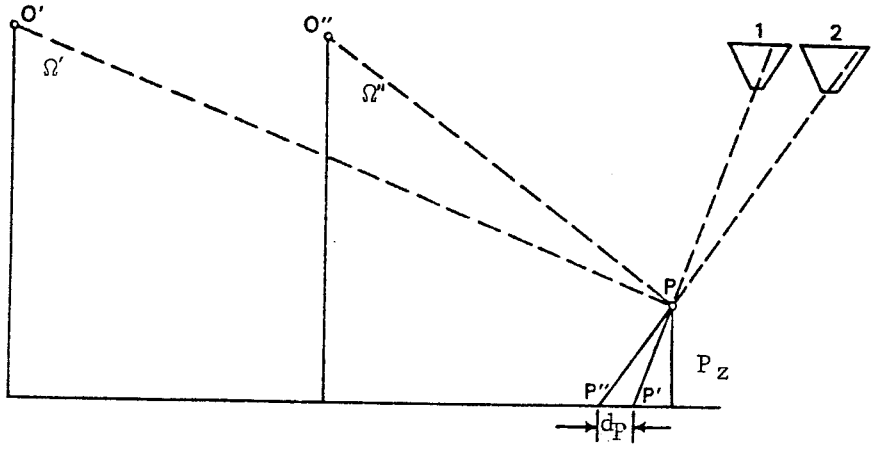

FIGURE 4: Relating an object height h to an observed parallax difference, dp, in ground range presentation.

Rather than deriving an appropriate formula from Eq. (11) we read directly from Figure 4, replacing the actual projection circle by a tangent at the object point:

$$p' = p_z \cdot \cot\Omega'$$

$$p'' = p_z \cdot \cot\Omega''$$

$$dp = p'' \pm p' = p_z \cdot (\cot\Omega'' \pm \cot\Omega')$$

$$p_z = dp \,/\, (\cot\Omega'' \pm \cot\Omega') \qquad (14)$$

where the "+" sign applies to opposite and the "-" sign to same-side stereo.

A discussion of these concepts is by La Prade (1963, 1970), Rydstrom (1968), Koopmans (1974), Derenyi (1975).

2.3.4 Judging Radar Stereo With Exaggeration Factors

An evaluation of radar stereo quality can be reached by judging the relative vertical exaggeration of height differences in the object. La Prade (1975) discussed the concepts and transferred them from photography to radar. When in photography the vertical exaggeration is about 3, this can also be obtained with radar. However, the figure in itself is misleading since it does not relate exaggeration to geometric resolution. The vertical exaggeration was a central issue in a paper by Leberl, Raggam and Kobrick (1985).

2.3.5 Judging Radar Stereo With Geometric Error Modelling

Theoretical radar stereo error studies were performed by Rosenfield (1968), La Prade (1970) and Leberl (1972b, 1978a, 1979). They relate an error in an element of exterior orientation in the left or right image to the resulting error of the stereo model coordinates. One can carry this further to the errors of distances, height differences and angles etc.

A full description of the derivations of all error factors is beyond the scope of this review. The necessary material is, however, fully documented in an earlier report (Leberl, 1979).

Height differences and cross-track distances are less affected by these errors than are coordinates themselves. To present but one example, assume a flight height H of 10 km, stereo base B of 8 km, $\Omega' = 68$ degree and $\Omega'' = 60$ degree. An error of the stereo base, dB, of 100 m will alter the p_y-coordinate by 233m, the p_z-coordinate by 577 m. But the same base error will affect an observed height difference of 1 km only by 50m.

The essential limitations of stereo radar are caused by random range errors $\sigma_{r'}$, $\sigma_{r''}$. In an aircraft stereo model of the above type errors will be caused by $\sigma_r = 10$ m with a σ_{py} of $\pm$ 42 m and with σ_{pz} of $\pm$ 70 m.

Clearly satellite radar is less appropriate for stereo operations if the same look angle applies in both images; this leads to very small convergence angles $\Omega' - \Omega''$ or a small stereo base, B. Satellite radar can, however, be used

for good stereo if two different look angles Ω', Ω'' are realized in the two orbits.

2.3.6 Generation Of Terrain Contour Lines

Hockeborn (1971) reported on the first radar mapping effort that resulted in (preliminary) contour lines of a previously unmapped area. Norvelle (1972) developed a computer program package to draw contour lines on a computer controlled photogrammetric stereo plotter. Leberl (1976a) presented contour lines of a lunar feature using Apollo 17 stereo radar. Yoritomo (1972) and Graham (1972) both reported on a technique to create digital topographic height data with both stereo and single flight interferometric radar techniques. This method has subsequently not been pursued. But it was also evaluated by DBA Systems (1974) without reference to contouring.

The use of radar for height mapping has thus been discussed and demonstrated on several occasions. However, stereo radar was motivated more by its significance for photo-interpretation than for contouring. The acquisition of terrain heights as a final product is expected to be only meaningful in special cases (planetary exploration such as of Venus), or if the sensor position and attitude measurements can be performed with sufficiently high accuracy such that the resulting stereo heights present an accuracy that is meaningful. This would be the case if 20 m contouring were feasible, corresponding to errors of individually measured points of about $\pm$ 7 m.

2.4 Blocks Of Overlapping Images

A block of images is a set of more than two overlapping radar strips.

The problem exists to radargrammetrically generate ground coordinates of objects based on:

- image coordinates of homologue points in all images that show there point;
- ground control points;
- tie points containing overlapping images;
- possibly sensor orientation and position parameters.

Mapping with a block of images is currently used in operational mapping projects. It was described in detail by Leberl (1975c, 1975d). It corresponds to methods in photogrammetry and photographic image block adjustment.

More rigorous and even three-dimensional (x, y and z) methods of radar block mapping were discussed by DBA-Systems (1974) and by Dowideit (1977). The sensor parameters of exterior orientation were described by polynomials or Fourier series. However, the demonstrated performance was limited to sets of three small image segments. The robustness of the technique was not discussed.

No further work has been reported on radar blocks, essentially because radar image block mapping is rather rare and therefore does not justify sizeable research and development efforts.

3 PAST EXPERIMENTS

3.1 Single Radar Image Accuracy

Numerous authors have compared single radar images to maps, thereby employing one of the described computing methods. An example of an early effort was by Leberl (1972a). Various interpolative methods were used to describe the image deformation.

Table I is a review of some existing work. In view of the many possible mapping methods, of variations in the image types, of input data available on the terrain etc., it is obvious that a comparison of results is nearly impossible. However, one conclusion can be drawn, the range of achievable results stretches from the geometric ground resolution (Gracie et al., 1970) to some large figures. Clearly, though these larger figures may be caused by unknown topographic relief, lack of ground control points or poor internal geometry.

Expectations were expressed in the preparation phase of satellite radar that it could result in higher image geometry performance than aircraft radar (Leberl, 1976b). SEASAT-SAR was the first data to potentially prove that expectation. However, the overall system engineering for SEASAT-SAR did not optimize geometric performance. Table II presents geometric accuracies obtained with SEASAT-SAR. Hardcopy images on film either from optical or from digital correlation provided the same accuracy. Time and range referencing was not of sufficient quality to fully capitalize on a relatively stable orbit geometry and the resulting good geometric potential (Leberl et al., 1981). Without any ground control no meaningful positioning of ground points was feasible. With one or two such points the positioning error is $\pm$ 300 to 400 m.

For SIR-A errors are reported by Kobrick, Leberl and Raggam (in print) to amount to about $\pm$ 100 m.

TABLE I

Single image radargrammetric performance results (from Leberl, 1976b)

Source	Year	Accuracy (meters) along 1σ	Accuracy (meters) across 1σ	Relief	Control per 100 km²	Resolution (ground-meters)	Antenna Stabilized	Antenna Type	Radar system code	Scale of images 1:	Area designation, remarks
Gracie	1970	20	14	Flat	10.0	17	Yes	Synth.	AN-APQ 102		Atlanta, Georgia
Leberl	1971	50	23	Flat	10.0	30	No	Real	EMI (U.K.)	200 000	Netherlands
Bowman	1971	47	60	Flat	10.0	30	No	Real	EMI (U.K.)	250 000	Netherlands
Konecny	1972	152	255	Mount.		17	Yes	Real	Westinghouse	216 000	N. Guinea – conf transformation
Greve	1974	35				⩾3	Yes	Synth.	TOPO II	100 000	Dig. monoplotting
Goodyear	1974	38	30	Flat	3.0	12	Yes	Synth.	GEMS 1000	400 000	Phoenix, Arizona
Derenyi	1974	89	111	Hills	1.1	17	Yes	Real	Westinghouse	250 000	Washington, D.C.
DBA-Systems	1974	51	26		0.5	3	Yes	Synth.	AN-ASQ 142	100 000	Radar interferometer
Konecny	1975	80	79	Flat		12	Yes	Synth.	GEMS 1000	400 000	Phoenix – conf transformation
Derenyi	1975	30	28	Flat		12	Yes	Synth.	GEMS 1000	400 000	Phoenix – control density not spec
Tiernan	1976	209	257	Flat	0.7	30–150	No	Synth.	Apollo 17	1 Mill.	Lunar satellite
Leberl	1976	147	233	Flat	0.3	30–150	No	Synth.	Apollo 17	1 Mill.	Lunar satellite
Hirsch	1976	120		Flat	3.0	30	No	Real	EMI (U.K.)	100 000	Netherlands
Leberl	1976	140	190	Flat	0.3	25–150	No	Synth.	JPL L-band	500 000	Alaskan tundra – sat. radar simul.

TABLE II

SEASAT-SAR geometric accuracy. Coordinate errors in km after radargrammetric measurements and computation, using the arctic passes over Banks and Victoria Islands taken by SEASAT covering 35 000 km², and pass 351 over Los Angeles

No. of control points	Rigorous radargrammetry x	Rigorous radargrammetry y	Simple scale fit x	Simple scale fit y
Sea arctic images of Banks Island, 35 000 sq km				
1	0.45	0.49	—	—
2 (at both ends)	0.33	0.26	0.37	0.37
17	0.17	0.16	—	—
Image over Los Angeles, 7 pts per 100 sq km				
Optical corr.	0.024	0.017	—	—
Digital corr.	0.022	0.012	—	—

3.2 Stereo Imagery

Table III is a compilation of radar stereo results obtained by various authors in the past. A definite quantitative conclusion on stereo accuracy is not possible at this time, the variation of the results is caused by the fact that various systems were used: with/without antenna stabilization; with low/high flying aircraft; in/outside atmospheric turbulences; and with low/high density of ground control etc. A conclusion can only be drawn to the effect that a great variation in achieved accuracies has been reported, ranging from the ground resolution up to many times the resolution. Controlled experiments would be required to obtain a more thorough appreciation of the influence of various parameters with real imagery.

TABLE III

Radar stereo accuracies obtained by various authors

Source	Year	Accuracy (meters)			Contol per 100 km²	Resolution (ground-meters)	Antenna		Radar system code	Remarks
		Along 1σ	Across 1σ	Height 1σ			Stabilized	Type		
Gracie	1970	12.2	7.7	13.2	35.0	17	Yes	Synth.	AN-APQ 102	Opp.-side
Konecny	1972	68.0	138.0	240.0		17	Yes	Real	Westinghouse	Opp.-side
		130.0	428.0	1548.0						Same-side
DBA-Systems	1974	26.8	21.9	16.7	1.2	3	Yes	Synth.	AN-ASQ 142	Opp.-side
		29.5	25.6	19.7						Same-side
Goodyear	1974			93.0	3.3	12	Yes	Synth.	GEMS 1000	Same-side
Derenyi	1975			33.0		12	Yes	Synth.	GEMS 1000	Opp.-side
				177.0						Same-side
Leberl	1975	173.0	510.0	109.0	0.3	30–150	No	Synth.	Apollo 17	Same-side, small base, satellite

Table IV summarizes more recent results. Stereo measurements were done with a stereoscope and parallax bar to obtain dp, with a digitizer to record r', r" or ', ", then with a photogrammetric stereo plotting instrument Planimat-D, which was used as a comparator to measure image coordinates x', y', x", y".

TABLE IV

Accuracy comparison for various stereo models, using simple parallax measurement techniques

Area	Type of radar	Figure number	Type of measurement	Number of points used	Height error (m)	Correction polynomial
Granite Mountain	Goodyear GEMS	30	Parallax bar	21	78 49	11 Coeff. 17 Coeff.
Granite Mountain	Goodyear GEMS	30	Stereoplotter	21	106 48	11 Coeff. 17 Coeff.
Granite Mountain	SEASAT-SAR optical	33	Parallax bar	28	96 121	17 Coeff. 11 Coeff.
			Stereoplotter	28	121 130	17 Coeff. 11 Coeff.
Los Angeles	SEASAT-SAR optical		Parallax bar	28	143 199	17 Coeff. 11 Coeff.
Los Angeles	SEASAT-SAR digital	34	Parallax bar	28	121 236	17 Coeff. 11 Coeff.

Table III leads to the conclusion that the results of aircraft radar with intersection angles of 6 degrees to 20 degrees produce height errors that are only somewhat better than those from SEASAT-SAR with intersection angles of 3 degrees to 5 degrees. The reason for the small differences is the fact that look angles with SEASAT are much smaller than with the aircraft data. This compensates to some extent for the poorer intersection geometry. The values conform to the theory. The SEASAT Los Angeles data are poorer than those from Granite Mountain, because intersection angles are more favourable in the latter case. There seem to be no differences between optical and digital correlations when the simple procedures were used that rely on stereoscope and parallax bar.

Most recently results have been developed for stereo from SIR-A: Kobrick, Leberl and Raggam (in print) report an accuracy in height of $\pm$ 160 m.

3.3 Radar Image Blocks

Numerical results from radar mapping efforts with image blocks exist using simulated data (Leberl, 1975d) as well as from operational projects, e.g. Brazil (van Roessel and de Godoy, 1974), in Colombia (Leberl, 1975c), and in West Virginia (Leberl et al., 1976). Simulated data permitted comparison on computational techniques leading to the conclusion that spline modelling is distinctly superior to other investigated methods on internal block adjustment.

In Brazil's RADAM no block adjustment was performed, but external control of each image flight with Shoran was used. The accuracies amounted to ± 0.5 km for a radargrammetrically computed point.

In Colombia's PRORADAM, images were flown with 63 percent sidelap. Tie-point transfer from one image to the next showed errors of ± 130 m in the terrain. The radar block deformations amounted to ± 2.2 km prior to correction. After adjustment an independent comparison with LANDSAT-satellite images demonstrated that radargrammetric coordinates deviated from LANDSAT-coordinates by about ± 400 m. This combines radar and LANDSAT errors.

A more complete numerical evaluation of a radar block was feasible with data from a well-mapped area in the USA. A 20 percent sidelap was generated of a 90 000 km^2 area in West Virginia. Tie-point transfer was accurate to within ± 25 m. A presentation of the radar block adjustment result clearly reveals that accuracies approximate ± 100 m, for control of 20 or so points per 100 000 km^2.

4 SUMMARY ON THE CURRENT UNDERSTANDING OF RADARGRAMMETRY

Previous chapters have reviewed the existing body of literature and experiments with radar imagery for mapping.

Currently available radar images have geometrical resolutions of about ± 3 to 25 m. They exist from aircraft and, in an experimental context, from spacecraft (Apollo 17, SEASAT and Space Shuttle SIR-A). Operational applications are for small scale 1:200 000 planimetric reconnaissance type mapping of previously unexplored areas, and for surveillance purposes in coastal and arctic environments. The geometric accuracy is not of great concern. It is the interpretation of image details that is the focus.

However, several radargrammetric concepts are of relevance today and may gain weight as and if radar increases in importance for remote sensing from both aircraft and satellites. These concepts are:

(a) providing a geographic location for each image point;

(b) rectifying a given radar image to generate a maplike ortho-radar-image;

(c) exploring and developing optimum radar stereo capabilities for enhanced image interpretation and the reconstruction of the third dimension of the object;

(d) assisting in the systematic and repeated coverage of larger areas with blocks of images and develop concepts to efficiently and rapidly convert them into maps;

(e) participating in the creation of real or near real time monitoring systems of rapidly changing phenomena, such as sea ice, coastal traffic etc.;

(f) processing of radar together with other data to create image synergisms and image-based information systems.

The work required depends on the further role that radar images are going to play for the observation of the Earth's surface and of other planets. Promises exist of future satellite radar (Space Shuttle SIR-B, Canada's surveillance satellite SURSAT, the European Space Agency's ERS-1, the Japanese ERS-1 and the NASA Venus Radar Mapping mission etc.), and of miniaturized, multi-frequency, all-digital aircraft SAR. If this indeed materializes, then clearly digital radargrammetry needs to be developed with rigorous mathematical models, aiming not merely at a fast and often improvized solution, but at the optimum radargrammetric performance.

The current perspective seems to point to an all-digital radargrammetry instead of today's hybrid techniques, where analog recordings on film are presented to an observer who then takes measurements that are

subsequently treated digitally. Radar sensors will be digital camera substitutes or complements, before the digital central perspective camera will be widely available. Therefore digital radargrammetry can obtain a role in the future that may carry more weight in relation to camera photogrammetry than it currently has.

Thus the main advances in radargrammetry must also be the incorporation of digital image processing technology into the image analysis repertoire. The improvement of geometric resolution, navigation parameter estimation and the wide availability are not the objectives of this field, but do affect it greatly.

An essential tool for radargrammetric method development and evaluation should be image simulation. There are several open areas of significance in radargrammetry that could benefit from the availability of digital image simulation systems. Such open areas are stereo-imagery, image rectification and mosaicking, multi-spatial data analysis and creation of image synergisms etc.

Within the field of general purpose mapping of planimetry, radar has played only a modest role so far, totally dominated by aerial photography. The situation is more distinct even regarding height mapping. However, new mapping tasks are emerging that previously did not exist.

Necessary efforts must continue to more fully explore areas that have been covered weakly in the past. An essential step is demonstration of capabilities with both simulated and real imagery that is available. Thus the next chapters discuss new methods developped to extract information from global scenes of digital (and partly also analog) radar imagery by using the already existing work in the field of radargrammetry as presented here. The influence of specific system parameters will be discussed by the practical approach of showing their effect on the output image through radar image simulation.

5 DEFINITION OF SPECIFIC APPLICATIONS

5.1 Specification Of Relevant Parameters And Their Effects For Geological Applications

The interpretation of radar imagery is influenced by system parameters, such as polarisation, wavelength, elevation angle and flight direction as well as target parameters, e.g. the electrical and physical properties of the imaged objects.

Effects of these parameters were studied by various authors by using radar image simulation to compensate the lack of real data: e.g. the effect of soil moisture on the radar radiometry by Ulaby et al. (1982); incidence angle considerations by Kaupp et al. (1982); the influence of sensor and flight parameters on the texture by Frost et al. (1984). Special requirements for system parameters and data processing steps for applications in geology are given by e.g. Bodechtel (1983); Jaskolla and Kaufmann (1984); Ford (1982); Blom and Daily (1982); and Frost et al. (1983).

In this study a limited number of system parameters were selected for a closer investigation, namely the elevation angle and the flight direction. Additionally a data processing technique for a geometric registration of radar imagery to other data sets (e.g. from maps) is proposed. Also a new processing algorithm to enhance non-linear features in radar imagery is introduced. The investigations, processing steps and results are documented in the following chapters.

5.1.1 Effects Of The Elevation Angle On Layover, Foreshortening And Shadow

The dynamic mode of imaging causes a lack of geometric fidelity in radar images, if for example compared to aerial photography. A closer investigation of relevant geometric parameters is called for due to the uniqueness of radar imaging principles. In non-flat terrain one has very peculiar effects of layover, foreshortening and shadows. Although at least shadows and foreshortening may exist also in other imaging principles, they are of a particular significance in radar since they effect the usefulness of the data.

Layover, foreshortening and shadows depend on the terrain relief (height, slopes) of the area to be imaged and the radar elevation angle at imaging time. The elevation angle is defined as the angle between a vector from the sensor position to the nadir and the line connecting sensor position and terrain point. For any height model, layover and foreshortening are high in the near range (steep elevation angles) and low in the far range. The opposite is

true for radar shadowing: High elevation angles create a bigger amount of shadow. Optimal elevation angles minimize these effects. For spaceborne imaging the value of the elevation angle between near and far range is quite constant (SIR-A: 47 deg $\pm$ 3 ; SEASAT: 20 deg $\pm$ 3.5). For airborne images the elevation angle varies much more and the undesirable effects of low or high elevation angle will be present in the image.

For discussion of the effects of the elevation angle on radar imagery five stripes of radar data from different sensor systems are compared. Fig. 5 presents an airborne radar image from the Granite Mountains by Goodyear with a high elevation angle of 63° to the first data point. Most data of the backslopes is lost in radar shadow. Fig. 6 presents another airborne radar image of the Grand Canyon starting at 11.3° off nadir: Strong layover predominates the image.

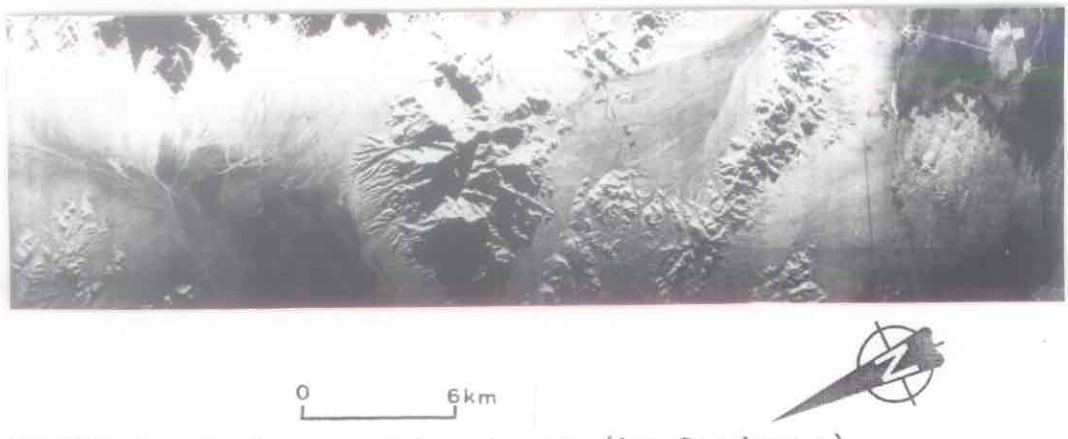

FIGURE 5: Airborne radar image (by Goodyear),
Granite Mountains
Elevation angle: 63 degrees
Imaging altitude: 12 km.

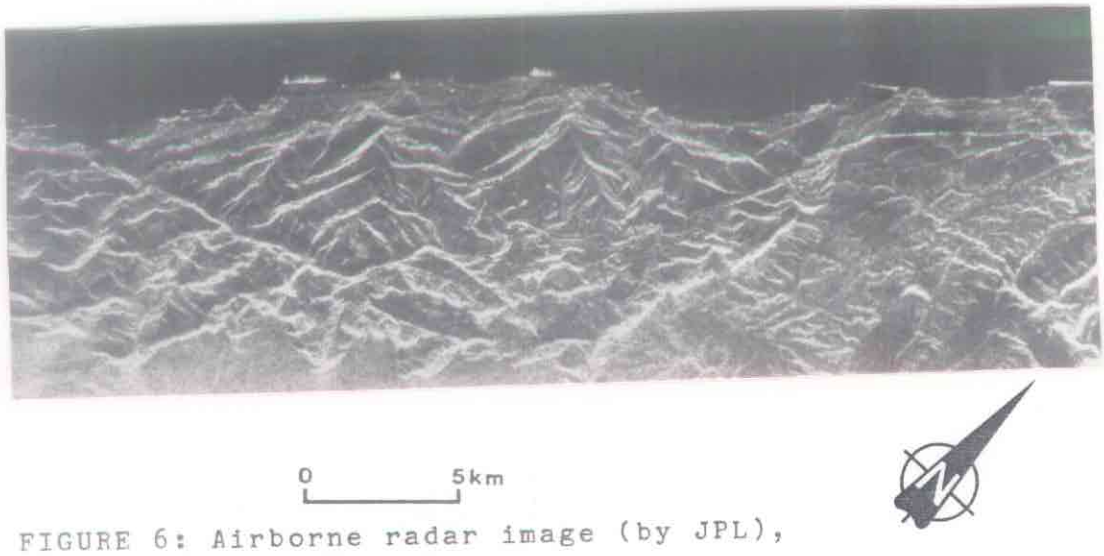

FIGURE 6: Airborne radar image (by JPL),
Grand Canyon.
Elevation angle: 11.3 degrees
Imaging altitude: 10 km.

Fig. 7 to Fig. 9 present spaceborne SAR images. The Appollo data and the Seasat data are both taken under very low elevation angles (5° and 17.5°, respectively to the first data point): again the images are characterized by strong layovers and foreshortening. The SIR-A data with 47° elevation angle off nadir shows neither layover nor shadow.

Thus the real data proves the significance of the elevation angle on the image quality, but is of no use for closer investigations in optimal elevation angles, as there is an additional variation in system and target parameters. However, data sets with varying elevation angles but fixed other parameters (including the area to be imaged) can hardly be found within the real data. Thus radar image simulation is chosen as a tool to investigate closer on this subject.

0 20km

FIGURE 7: Spaceborne radar image, Apollo 17 Lunar Sounder Experiment (ALSE).
Elevation angle: 5 degrees
Imaging altitude: 112 km.

0 15km

FIGURE 8: Spaceborne radar image (by SEASAT), Los Angeles.
Elevation angle: 17.5 degrees
Imaging altitude: 800 km.

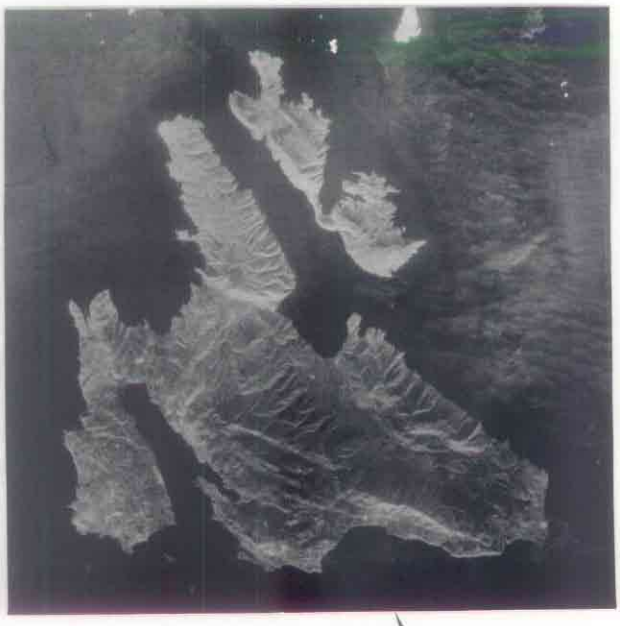

9a

0 10km

9b

FIGURE 9a: Spaceborne radar image by SIR-A,
Greek Islands Cephalonia and Ithaca.
Data Take 32-33.
Elevation angle: 47 degrees
Imaging altitude: 262 km.

FIGURE 9b: Spaceborne radar image by SIR-A,
Greek Islands Cephalonia and Ithaca.
Data Take 37a.
Elevation angle: 47 degrees
Imaging altitude: 262 km.

(a) Definition of the terms layover, foreshortening and shadow

Radar layover: The location of a point in the image is a function of the distance between sensor position at imaging time and corresponding terrain point. Therefore terrain features like steep mountains may be imaged "laid-over" in the near range: the peak of the mountain is imaged before its bottom. Practically the image will show two areas on top of one another.

Mathematically, layover occurs where the incidence angle (angle between vector from sensor position to target point and surface normal in target point) is negative. This is true, whenever the slope in the terrain exceeds the elevation angle.

Radar foreshortening: Compared to their real lengths in the

terrain, slopes appear usually shorter in radar images. This radar property is denoted as "foreshortening" and is also dependent on the incidence angle θ^i.

The percentage of radar foreshortening F_p is defined as

$$F_p = (1 - \sin \theta^i) * 100$$

This shows that the only time the slopes are imaged in their true length is at incidence angles of 90 degrees.

Radar shadow: Terrain surfaces in the imaged area that are not illuminated by the radar beam appear as "radar shadow" in the image. The image location of a shadow point does not show any signal since none was reflected from the corresponding object point. In contrast to photography, there is no diffuse illumination of shadow areas; therefore radar shadow areas carry no information whereas photographic images will usually show information also in shadow areas.

Backslopes are in the shadow, if the incidence angle passes 90 degrees. However, this criterion does not include surfaces hidden by other terrain features. A more general rule is that with increasing swath with elevation angle has to increase in order to reduce shadow in the far range.

(b) Calculation of image quality in terms of foreshortening, layover and shadow

We define the existence of layover, foreshortening and shadows as a loss of image usefullness. The extent to which the above mentioned radar properties effect the image can be calculated using the investigated radar image pixels. This is done by using the advantage of the simulator: To each synthetic image grey value additional information like incidence angles and a shadow indicator are stored. After completion of image simulation a simple calculation can be performed to sum up the percentages of the specific image distortions and shadows.

Figure 10 illustrates the radar imaging geometry in a plane perpendicular to the flight path, thus explaining layover, foreshortening and shadows.

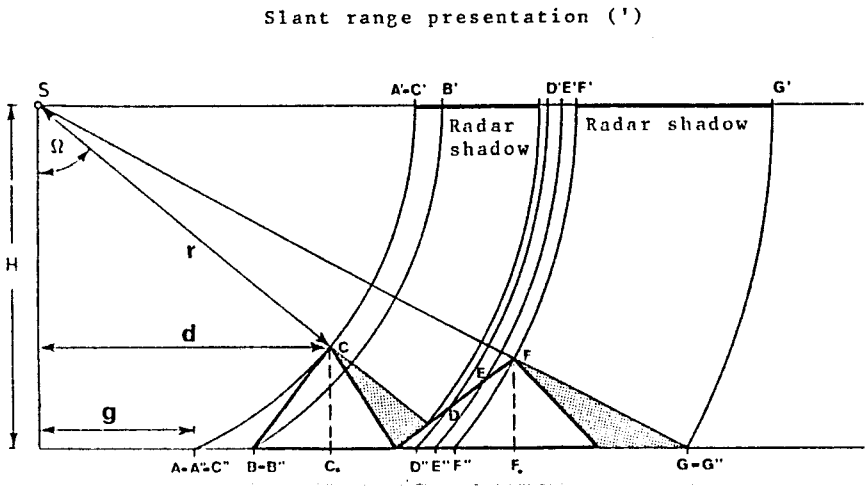

S ... sensor
H ... flight altitude
r ... slant range
g ... ground range
Ω ... elevation angle

A'=C' ... layover
$\overline{DE} > \overline{D'E'}$ ... foreshortening

FIGURE 10: Imaging geometry in a plane perpendicular to the flight path showing radar layover, foreshortening and shadow.

5.2 Effects Of Flight Direction To Enhance Linear Features In Radar Images

The presence of linear features (lineaments) in an area may indicate faults and fracture zones and might in cases give information on past or future movements within the earth's crust or indicate economically important environments. In radar images the lineaments trending perpendicular to the illumination direction, i.e. parallel to the flight path, are enhanced. Terrain structures which are reconstructed only from topographic imaging effects can be investigated by creating image simulations. With the help of a number of different flight paths all main linear features of the topography can be enhanced. The amount of flights and their intersection angles will be investigated in chapter 8.4 by using a specific test area.

5.3 Flight And Imaging Parameters To Create Radar Stereo-Pairs

The main use of radarstereoscopy lies in the improved interpretability. Another secondary application of radar stereo-pairs is the creation of digital elevation models. This might be necessary, where topographic maps are unavailable or only exist in very large scales.

A major issue is the viewability of same and opposite-side stereo-study. Studies for optimal stereo-configurations through simulation have been attempted previously, e.g. by Kaupp et al. (1982) and Domik et al. (1983). In a continuation of these efforts a mountainous test site (Sardegna) was investigated for optimal stereo-intersection angles for a configuration with same-side stereo at a given flight height, but with various elevation angles. No real same-side stereo-pair exists for Sardegna, therefore the study must be based solely on simulations.

During the SIR-A mission Sardegna was imaged twice by crossing flight paths at an angle of 16 degrees. This stereo-configuration (same elevation angle, crossing flight paths) proves to be sufficient for stereo-viewing and hence to improved interpretation. Unfortunately, the lack of quality in one of the investigated images (data take 37A) made it impossible to use the image pair also to create a sufficient DEM. General viewability limitations for this type of stereo-configuration are described in a report by Domik et al. (1983) using data from SIR-A over two Greek islands. Figure 11 describes these particular sets of stereo-configurations.

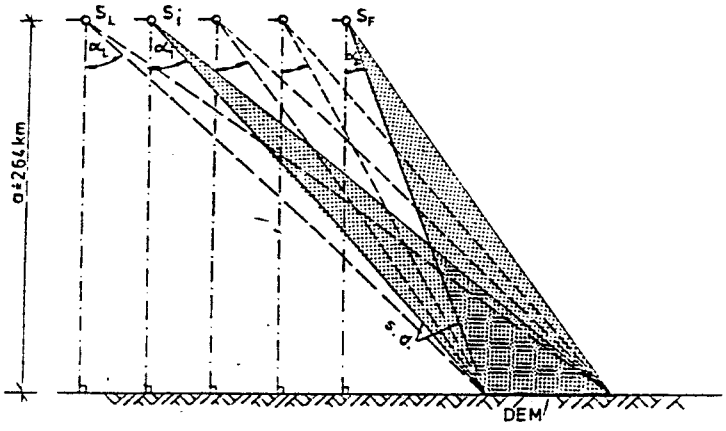

(a)

DEM ..... Digital Elevation Model
S_F ..... Satellite at first flight
S_L ..... Satellite at last flight
a ..... Altitude
s.d. ..... Sweep Delay
..... Elevation Angle

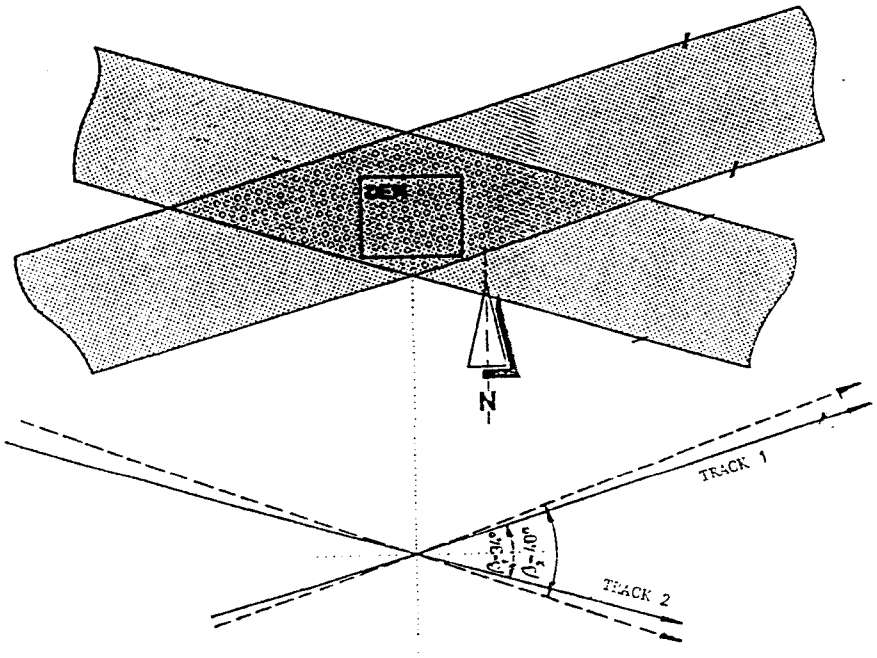

(b)

FIGURE 11: Setup for radar stereo-configurations:
(a) Same illumination direction and different angles.
(b) Different illumination direction and same elevation angle.

5.4 Proposed Processing Algorithm For Non-Linear Feature Extraction In Digital Images

The study area is not only covered by three radar images (SIR-A, SEASAT) but offers also a topographic map, a lithological map and a map with lineaments. Topographic maps were available in different scales and standard map projections. To combine these data with the radar images one of the following steps has to be performed:

a) Geometric rectification of the radar images to fit the map geometry

or

b) proper distortion of the map information to fit the radar geometry.

Usually geometric rectification of the radar image is done since this will match the image with a larger variety of collateral data. Also in the current case this option has been exercised through a multi-step rectification procedure, explained in more detail in chapter 7. This includes an image resampling step. Resampling may change subtle lineament data and reduce the ability to differentiate specific lithological classes in the image. Thus also step (b) - distortion of the lithological map to fit the geometry in the radar images - has been investigated and performed in this study.

6 TEST AREA SARDEGNA: AVAILABILITY AND QUALITY OF DATA

6.1 Data From Available Maps

(a) Elevation Model

For the creation of the digital height model 12 map sheets at a scale of 1 : 25 000 were available. The numbers and locations of the maps are indicated by dark grey tones in Fig. 12. The geographic coordinates of the covered area are:

left bottom corner Lat. = 40°00'00" North
Lon. = 9°19'38.4" East (of Greenwich)
right top corner Lat. = 40°20'00" North
Lon. = 9°42'08.4" East (of Greenwich)

The 25 m contour lines of the 12 map sheets were digitized, then discretizised and interpolated to a 100 meter x 100 meter raster. This raster was chosen to fit the resolution of the radar images.

An axonometric view of the digital elevation model is shown in Fig. 13; and the reinterpolated contourlines of the area as shown in Fig. 14 to illustrate the ruggedness of the study area.

Program systems available at the Institute for Image Processing and Computer Graphics were used to create the elelvation data. These programs include:
DESBOD for digital compilation, storing and processing of spatial data; it served to digitize the contourlines.
Program GTM (Graz Terrain Model) actually performed the discretization of lines and interpolation of elevations in a grid.

(b) Geological Map

The study area is covered by a geological map at a scale of 1 : 25 000. Relevant parts were digitized for further investigations. Fig. 15 and Fig. 16 show the digitized lineaments and lithological classes.

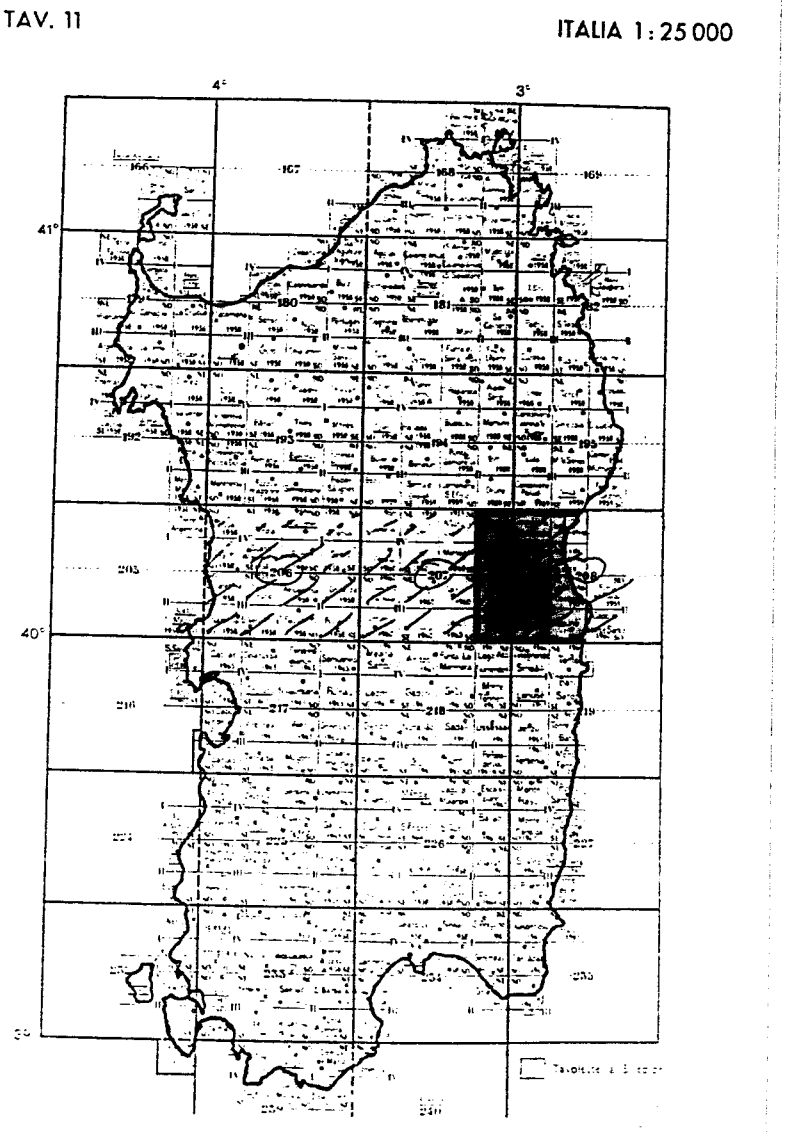

FIGURE 12: The numbers and location of the maps used to create a digital elevation model of the Sardegna test area. Note: Longitude refers to the national Italian reference system.

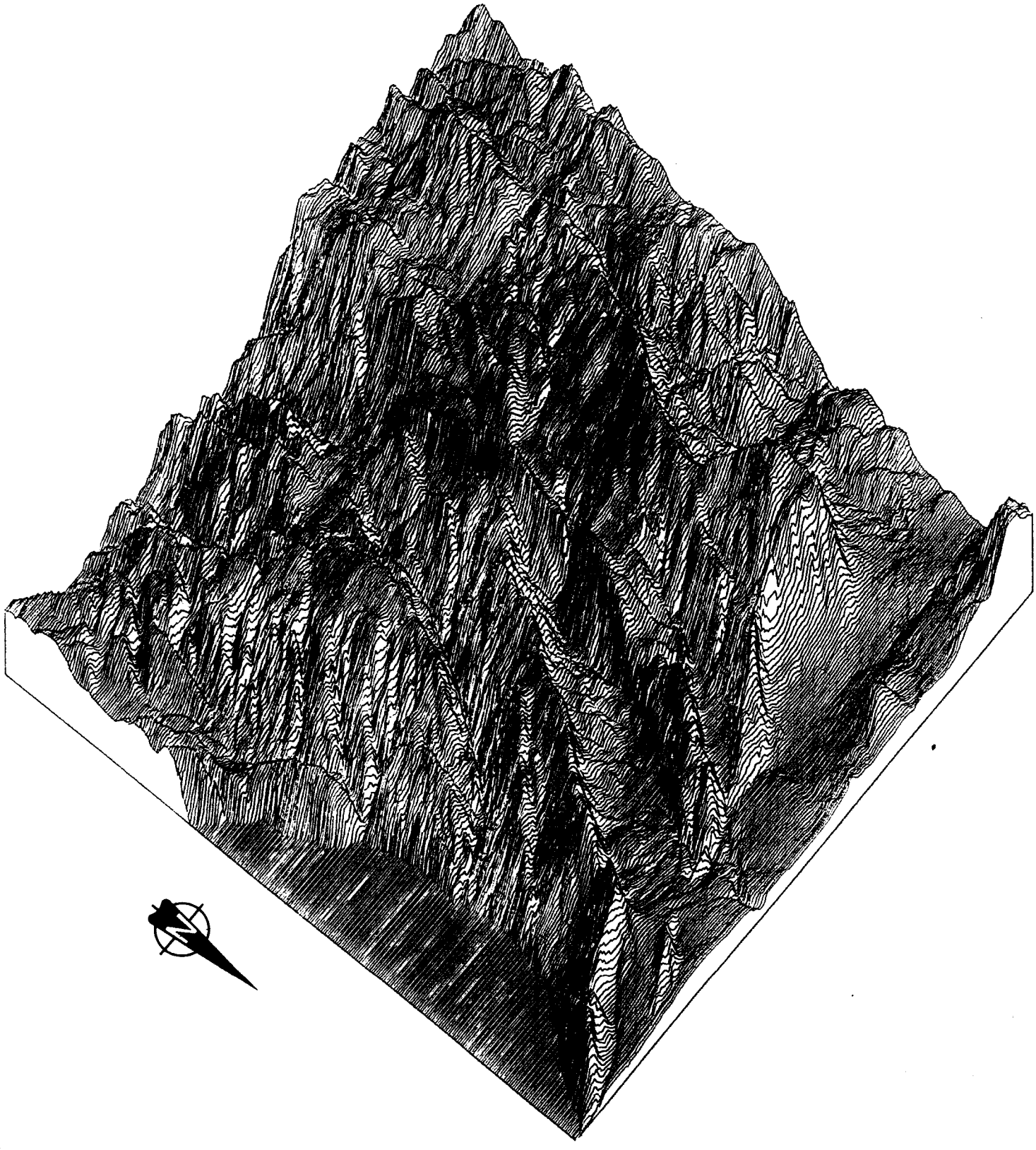

FIGURE 13: Axonometric view based on the digital terrain model of the test area Sardegna.

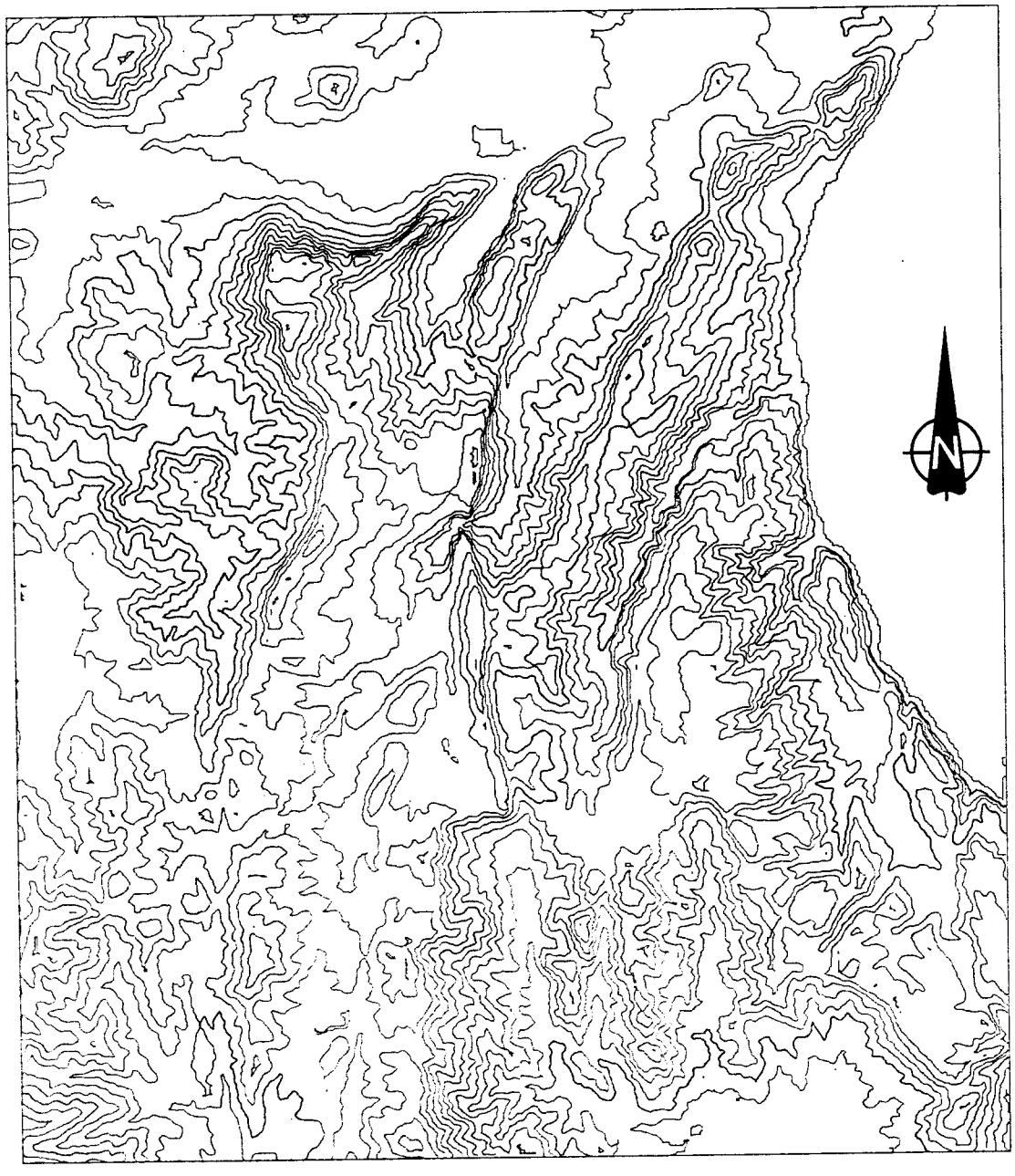

FIGURE 14: Reinterpolated contour lines of the original data derived from scanned contour lines for generation of the digital terrain model.

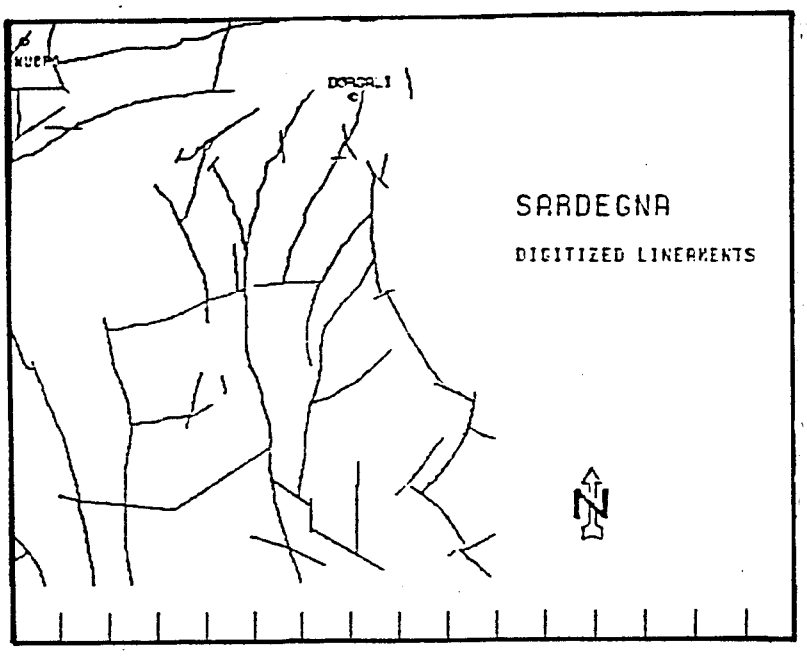

FIGURE 15: Lineament map of the test area Sardegna. One unit of bottom scale corresponds to 3.2 km.

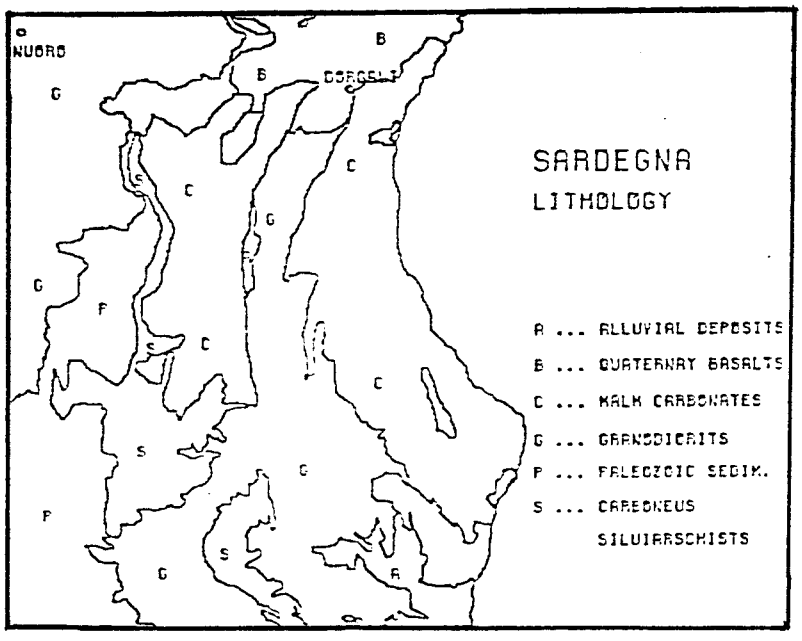

FIGURE 16: Lithological map of the test area Sardegna. Same scale as in Figure 15.

6.2 SIR-A Images:

During the second shuttle flight in November 1981, a side looking radar experiment to aquire images for investigations for natural resources mapping was carried out. This Shuttle Imaging Radar-A (SIR-A) experiment resulted in approximately 8 hours of imaging radar data in 25 data acquisition periods. The data was processed optically at the Jet Propulsion Laboratory (JPL). A nominal ground resolution of 40 meters was obtained.

Parts of the island Sardegna, Italy, were imaged twice during this experiment: once in data take 35-36, orbit 30 and once in data take 37A, orbit 31. The images were available on film and digitized by an Optronics device for further processing. The digitizing resulted in a pixel array of grey values, where each pixel presents approximately an area of 11 m square. By averaging the values to remove the speckle effect, a pixel size of 100 m square was created (Fig. 17). This rather low geometric resolution was desired to enhance image quality. As a by-product the specific test area was thereby made to fit into the refresh memory of a 512 x 512 pixel DEANZA image array processor IP 6400.

Digital image analysis is based on accurate radar image simulation. This requires that flight and imaging parameters are available.

Given were (Cimino and Elachi, 1982):

- The swath center (latitude, longitude) and the imaging altitude at minute intervals. This is not quite sufficient for the Shuttle velocity of appr. 9 km/sec., and corrections had to be made for the flight path over the specific test area.

- The elevation angle for imaging at app. 50 degrees to the center of the swath.

- STC position and pulse rate frequency (PRF) to allow a closer derivation of the sweep delay time to the first imaged data point. (see "Mission Operations Procedure Handbook", 1981).

FIGURE 17a: Digitized SIR-A image, Data Take 37A.
Averaged by a factor of 9.

FIGURE 17b: Digitized SIR-A image, Data Take 35-36.
Averaged by a factor of 9.

The above-mentioned parameters and the values used in the simulation are summarized in Table V.

Table V
Parameters of Data Take 37A and 35-36

Data Take	37A	35-36
Flight altitude (km)	261.54	261.21
Satellite flight direction	81.073° clockwise from North	97.034° clockwise from North
Elevation angle to 1st data point	45.564°	45.637°
Sweep delay (km)	373.58	373.58

6.3 Seasat Images:

Seasat was launched in 1978 in a circular orbit with an inclination of 108° and an average altitude of 795 km above the earth. Even during its short functioning period (106 days) the synthetic aperture radar on board provided a large amount of data. Two scenes of Sardegna's east coast were digitally processed by the DFVLR and available for the study.

The processing resulted in digital arrays with a pixel resolution of 12.5 m and a radiometric resolution of app. 5500 density levels. Unfortunately the preprocessing in the geometry of the image made it more difficult to relate this data precisely to the existing height model and thus to the other images. Therefore this data could not be analyzed digitally as it was done with the two SIR-A scenes. Uncorrected data was ordered from JPL/NASA but did not arrive until the end of the investigations (Fig. 18).

One clear difference between Seasat and SIR-A images is the look-angle off nadir and the resulting geometric properties of the images. Seasat data contain layovers but no shadows; SIR-A has hardly layovers nor shadows.

FIGURE 18: SEASAT image showing southern part of the test area

7.0 PROCESSING ALGORITHMS

The processing algorithms used for the investigations proposed in section 5 and the preparation of the data sets are described in the following section.

The algorithms are based on the mathematical formulations and theoretical understanding of radargrammetry as they are presented in the first part of this study.

7.1 Radar Image Simulation

Approaches to image simulation can be categorised according to the domain of the transformation function. Object space algorithms map each object point (DEM point) into a two dimensional field (image) whereas image space algorithms start from equidistant image coordinates (i,j) of the output image and assign grey value accordingly to it. Object space algorithms are usually faster in their application than image space algorithms. But there is a need for interpolation to convert the unequally spaced image addresses to equidistant ones.

Grey values are attached to the image coordinates dependent on the corresponding incidence angle on the ground.

Fig. 19 and 20 show the basic idea of object vs. image space algorithms.

The more complicated, but also the more accurate approach - the image space algorithm - is discussed in more detail by Domik et al. (1983) and briefly on the following pages for ease of reference.

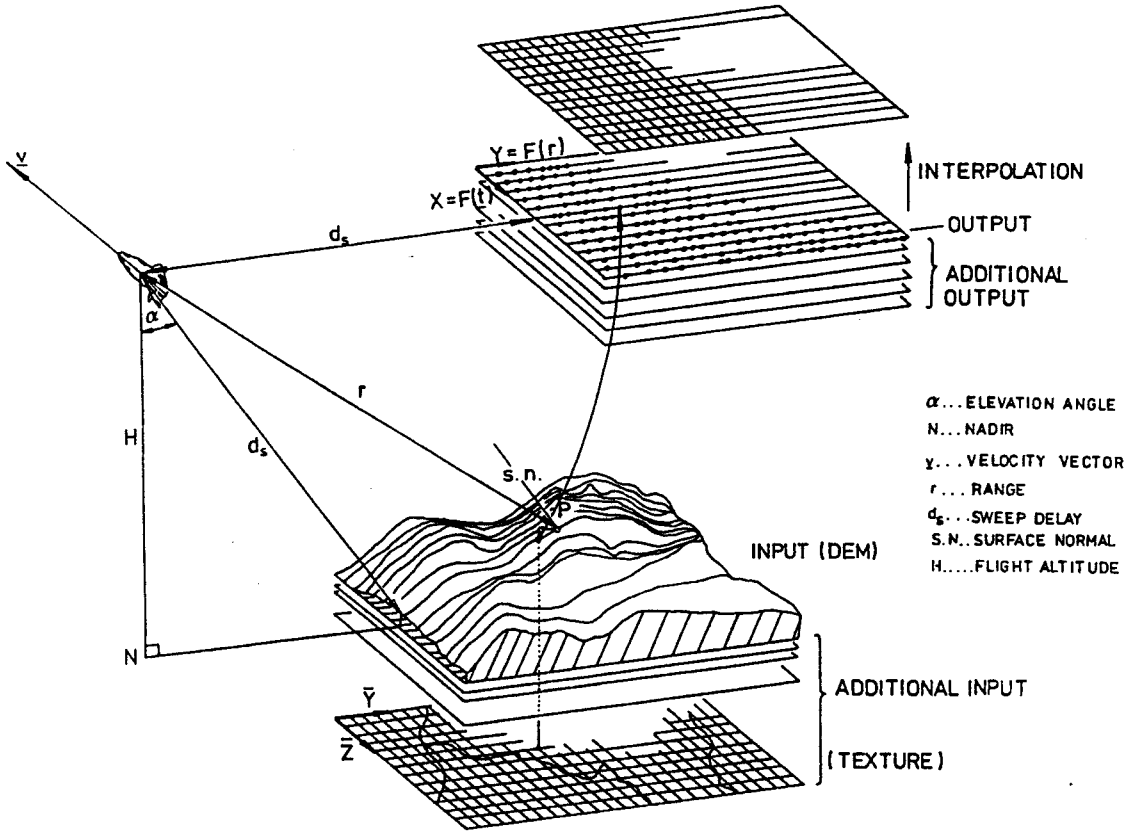

FIGURE 19: Graphic presentation of object space algorithm

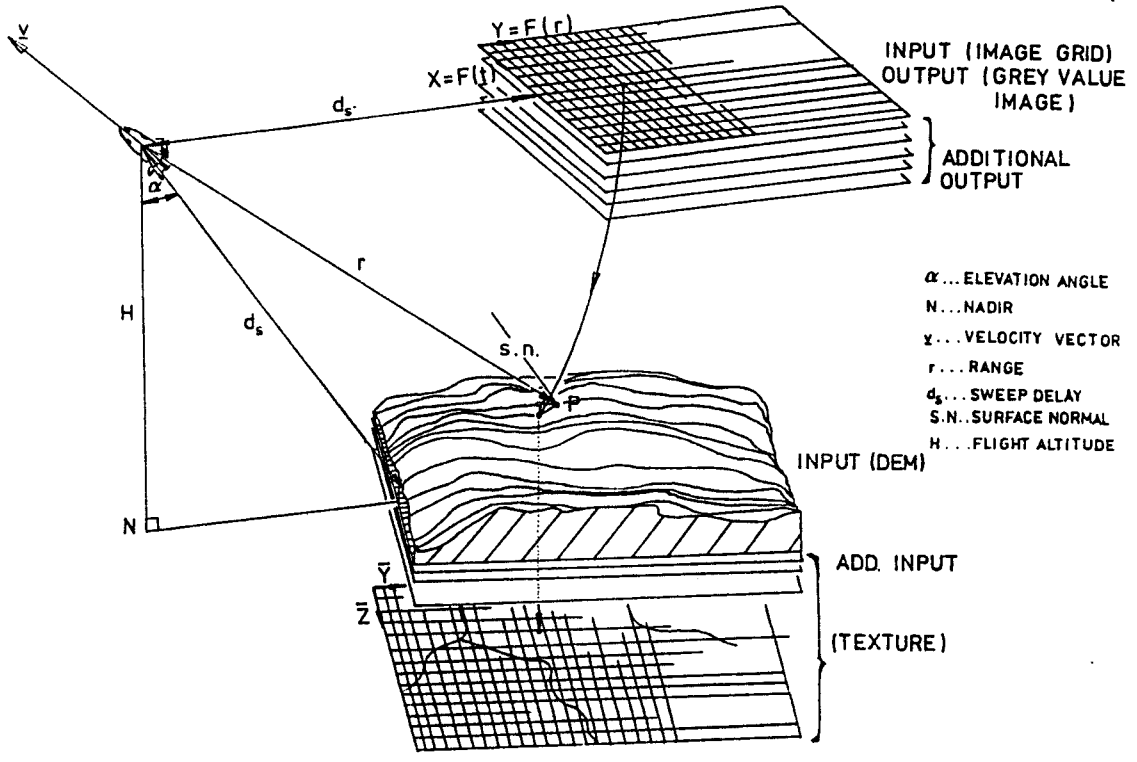

FIGURE 20: Graphic presentation of image space algorithm

7.1.1 The Geometric Imaging Model

The image coordinates (i,j) serve as start values for the simulation program. They are used to extract imaging time t and slant range r or ground range g by means of Equations (15):

$$t = (i-1)*f_i + t_0 \qquad (15.a)$$

$$r = (j-1)*f_j + d_s \qquad (15.b)$$

$$g = (j-1)*f_j + d_s \qquad (15.c)$$

$$r = SQRT(H^2 + g^2) \qquad (15.d)$$

where

t....imaging time of coordinate (i,j)
t_o...start time of imaging
f_i...scale factor in azimuth-direction
f_j...scale factor in range-direction
d_s...sweep delay

The sensor position and velocity vector, derived from the imaging time, define a cartesian coordinate system: The sensor position is the origin of this "sensor coordinate system", the axes are defined by the velocity vector and the sensor position as expressed in a geocentric coordinate system. The set-up of this system allows a clear presentation of the geometry created by any input coordinate (i,j). (see chapter 2.1).

The origin of the sensor coordinate system is the center of a sphere with radius r (range sphere). In general, a squint angle different from zero is assumed for imaging. Thus a cone is defined with the peak in the origin and its axis along the velocity vector of the air- or spacecraft. All generating lines form an angle with the axis of 90° minus squint angle. If the squint angle is equal to zero, imaging is in a plane perpendicular to the velocity vector. The intersection of sphere and cone, or, sphere and plane, respectively, defines a circle (intersection circle). The remaining task is now to intersect the circle with the DEM.

At least one but possibly several intersection points will be found. The occurrence of more than one solution is called "lay-over": different terrain targets were illuminated simultaineously. The address of each intersection point as well as corresponding look angle, surface inclinations and additional information are stored for further processing.

7.1.2 Radiometric Model Of Imaging

The definition of an image grey value in a given pixel location is denoted as "radiometric model". One has to define areas of shadow (black), diffuse reflection, multiple reflection in lay-overs etc.

Black image areas are mostly shadows or smooth water bodies. In order to find those pixels that indeed are shadow areas one has to sort the look angles going from near range to far range along an imaged object line. Shadow areas begin where an increasing range r is associated with a decreasing look-angle off nadir.

In areas other than shadows the image grey value is a function of the incidence angle for the incoming radiation. This is an angle between the line of sight antenna-object and the local normal onto the surface.

Once this angle is computed for a pixel one has the choice of selecting a backscatter curve according to the thematic charactaristics of the material and of the reflection angle. Standard backscatter functions are those of Hagfors (1964), Muhleman (1964) or a cosine-function.

Simultaneous illumination of various terrain parts leads to image lay-overs: the projection circle intersects more than one point on the ground. The grey value is the sum of the individual reflection values.

7.1.3 Data Structure

The internal data structures are constructed to make available a fast access to the address file elements in relation to the image elements. Each azimuth line in the image represents a logical block and corresponds to a unique logical block of the address file. Memory allocation for each logical block will be a minimum of ne bytes, where n is the number of range columns and e the number of bytes used for storage of one grey value. The address file allocates (at minimum again) hf bytes, with h being the number of addresses belonging to one azimuth line and f the number of bytes used for one address definition. The relation is realized by an additional access-matrix (pointer file), which allows a fast association between elements of the two different files. The additional storage for the relation matrix will be h2 bytes per logical block.

7.1.4 Software Implementation

The above described algorithm was implemented at the Institute for Image Processing and Computer Graphics on a VAX-11/750 under the name of SIMRISA (SIMulation of Radar images using an Image Space Algorithm). Emphasis was put on

modularity of the system (see description of system modules, Fig. 21). The program can be easily changed, e.g. additional thematic input data sets could allow for use of different backscatter curves or use of different look-up tables within one DEM area. Also a limited but fast version of an object space algorithm (named SIMROSA) was created and implemented. It operates on simpler assumptions than SIMRISA, but for investigations where certain parameters (e.g. squint angles) need not be studied, the results prove to be satisfactory.

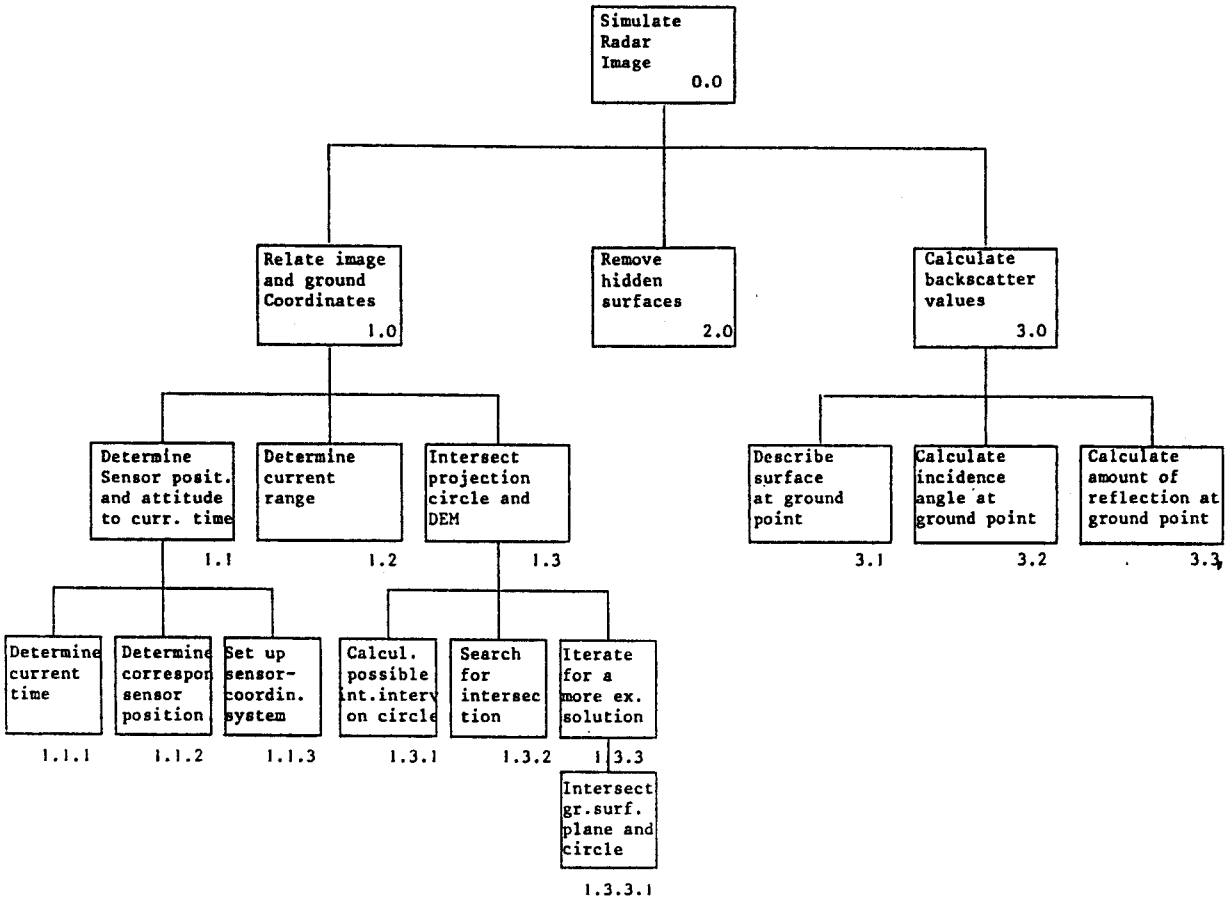

FIGURE 21: Modules of program system SIMRISA

7.2 Image Registration

The image registration is based on a program RECTIF by Diarra (1982); it is a modular software system for geometric correction of an image. Input is a set of homologue pairs of points whose coordinates are known in the real image and in the simulation. These are used to compute correction polynomials to describe the trend of the image

deformations. Residuals at control points serve then to compute refined corrections with some higher order interpolative method. Work is thus via "warping" or "rubber-sheeting". Polynomials are limited to degree 3 or less, so that they are both stable and overdetermined. Residuals are extracted at each anchor point, and serve to modify the original polynomials.

These correction polynomials are used for resampling based on a grid of anchor points; each set of object coordinates obtains image-positions. Various methods may then be applied to determine grey values at those positions: interpolation followed by nearest neighbor assignment, bilinear interpolation, and bicubic interpolation, are the current options. Control points will usually be defined by hand, or by digital correlation.

The registration results in a rectified image. In the case of data actually studied, remaining distortions amount to an average of 3 pixels or less, assuming an appropriate distribution of control points.

7.3 Radar Rectification Based On Simulation

The procedure used for the rectification of radar images of mountainous terrain consist of the following steps:

(a) Generation of a digital elevation model, either from a map or from other external sources, or from radar stereo mapping;

(b) Verification and improvement, or computation of, sensor position and attitude parameters based on identifiable ground control points;

(c) Using the outputs of steps (a) and (b), i.e. a DEM, radar imaging parameters and a flight path, create a simulated radar image to resemble the given input image;

(d) Correlate the real and the simulated radar image, either by pointing to homologue features or by automated correlation, thereby creating a grid of anchor points in the real radar image to relate to the simulated one and consequently to the object coordinate system;

(e) Using a warping function, correct the real image to fit over the simulated image;

(f) Generate a geometrically rectified real image by assigning the real image grey values associated with the simulated pixels to the corresponding DEM grid cells;

(g) By substraction of the real image grey values from the simulated image one obtains a radiometrically corrected output image.

The above steps imply that a radar image processing system and an extensive software are available. In fact, the system needs to consist of various separate elements. In the current context one uses:

- DEM generation by the Graz Terrain Model (GTM) system which takes given map contour lines to create a raster DEM;

- System for stereo mapping with radar techniques (SMART) to extract contour lines or raster DEM data from stereo radar imagery on a photogrammetric analytical plotting machine (Kern DSR-1);

- Radar space resection programs to compute the flight parameters from a given input image and ground control points;

- Image processing programs for image correlation display and coordinate extraction;

- General purpose rectification based on a grid of anchor points (Chapter 7.2);

- Radar image simulation (Chapter 7.1);

- Assignment of grey values to DEM grid cells based on an address file as a result of correlating the real with the simulated image.

The large set of required software for this purpose was evolved over the years in a sequence of individual efforts.

For an overview of data and programs see Figure 22.

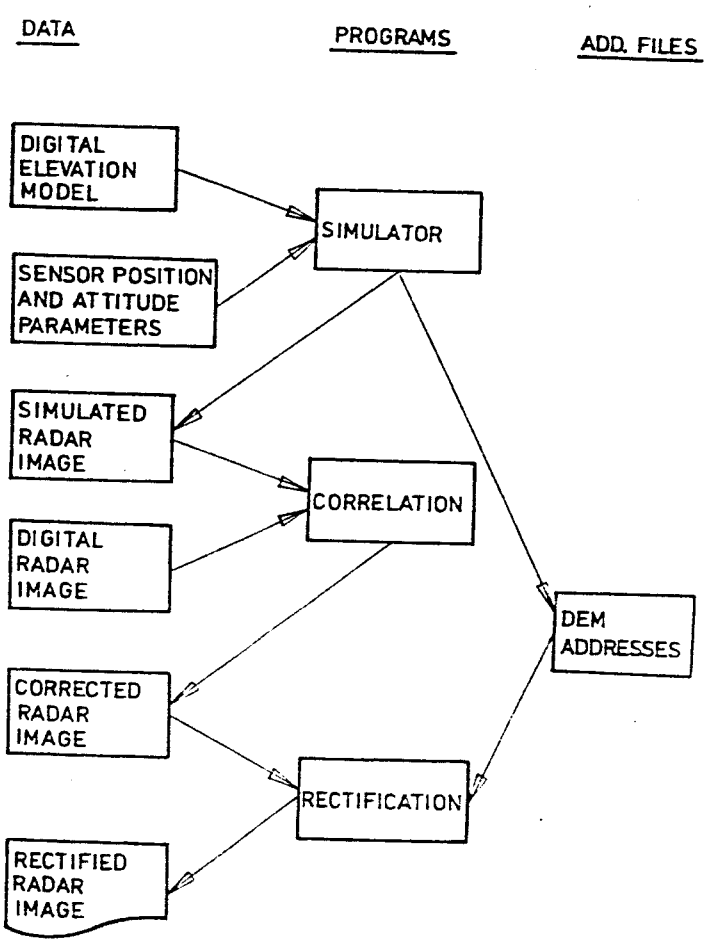

FIGURE 22: Programs and data flow of rectification procedure

7.4 Generation Of A DEM With Radar Stereo-Mapping

7.4.1 Background

Modern photogrammetric analytical plotters have opened up the possibility to employ other types of images than metric aerial photography for stereo-plotting. Instead of a fixed mechanical or optical analogon for the projection ray one has a flexible computer to relate image xy-coordinates to the cartesian XYZ object or model system.

Norvelle (1972) probably was the first to actually program an analytical plotter for stereo-radar. The flexibility of earlier analytical plotters was hampered by the available computers and the use of low-level programming languages. Prior to Norvelle's work stereo-radargrammetry was developed in the context of basic studies, e.g. by Rosenfield (1968) and Gracie et al.(1970), and had led to a rather unique and specific radar stereo-mapping instrument

(Yoritomo, 1972; Graham, 1972).

The current generation of analytical plotters employs general purpose computers, distributed processing and high level programming languages. Therefore the effort required to program them is much reduced when compared to the early systems. This fact is combined with an increased interest in radar remote sensing as documented by satellite and other radar imaging experiments. Therefore it appears increasingly meaningful to study radar stereo-mapping.

In an effort to demonstrate the flexibility of current commercial analytical photogrammetric instruments and in order to explore more fully the capabilities and limitations of stereo-radargrammetry a procedure and software system for the analytical plotter Kern DSR-1 was developed to set-up, and plot from, radar-stereo models. It is named SMART -- Stereo Mapping with Radar Techniques (Raggam, 1985).

This section will discuss the procedure and demonstrate it with a specific data set. Common radar image acquisition is performed with parallel flight lines. It is means an added complexity to use intersection flight lines. As will be shown, the DSR-1 is able to handle this type of data and produce a digital terrain elevation model of an accuracy commensurate with the radar input.

7.4.2 Overview Of System Modules

The main menu of the program system for stereo radar is shown in Figure 23. It can be seen, that it is organized in several separate modules. The entire process of model set-up follows radargrammetric formulations presented earlier and reviewed by Leberl (1983). Essentially the procedure requires sufficient ground control for the transformation of radar coordinates to the object space. The individual images are processed first to obtain approximate values for the rigorous radargrammetric solution. In the terminology of classical photogrammetry one first solves resections in space for the two images to then continue with a bundle adjustment using both images simultaneously.

```
                    S M A R T

PROJECT IDENTIFICATION = SHASTA

  START PLATE PROCESSOR          : 1
  PROJECT INFORMATION            : 2
  GROUND POINT MANAGEMENT        : 3
  ORBIT DATA MANAGEMENT          : 4
  SINGLE RADAR IMAGE             : 5
  RADAR STEREO MODEL             : 6
  ESCAPE                         <CR>
-------------------------------------
              DESIRED PROGRAM =
```

FIGURE 23: Main menu of program system SMART

In case no ground control should be available, one has to work with given or assumed parameters of flight path and sensor attitude. The preliminary resections would be skipped.

(a) Start plate processor: This module initializes, loads and starts the plate processor program.

(b) Information and Initialization Module: This task enables the input and manipulation of initial project and image parameters (menu see Figure 24). It serves for general information for the operator, such as for example project name, available images for the project or image and orbit data information.

(c) Control Point Management Module: This module is for the input and manipulation of ground control point data (menu see Figure 25). The ground coordinates are in an orthogonal cartesian coordinate system, usually referenced to an origin within the area to be mapped and the Z-axis pointing along the local vertical of the origin.

(d) Orbit or Flight Data Management Module: This is for input and manipulation of sensor position measurements (menu see Figure 26). The system assumes the orbit or flight to be represented with time polynomials so that sensor positions s may be expressed as follows:

$$\underline{s} = \underline{a} + \underline{b} * t + \underline{c} * t^2 + ...$$

where t is the time. Approximations for the orbit coefficient vectors ($\underline{a}$, $\underline{b}$, $\underline{c}$, ..) will be determined in the orbit data management module. Input are the position measurements, output is an array of polynomial coefficients. If need exists, joint low-order polynomials etc. will be used instead of higher order polynomials.

(e) Single Radar Image Processing: This module represents the equivalent of a resection in space to compute the orientation parameters for a single radar image with inner and exterior orientation (menu see Figure 27). Plotting with a single radar image may be done on either a spherical surface of chosen radius or in a three-dimensional X, Y, Z-coordinate system with known constant Z.

(f) Stereo Radar Image Processing: This module includes the actual set-up of a radar stereo model (menu see Figure 28). It is used subsequently to the single radar image module to determine approximations of the exterior orientation parameters of the two overlapping images. After elimination of y-parallaxes this module serves to plot contour-lines or planimetric features. Results are either directly plotted on an xy pen plotter or are entered into a digital data base for further processing. One example for the generation of digital terrain models is given by Oswald and Raetzsch (1984), where the currently operational Graz Terrain Model (GTM) program system is presented.

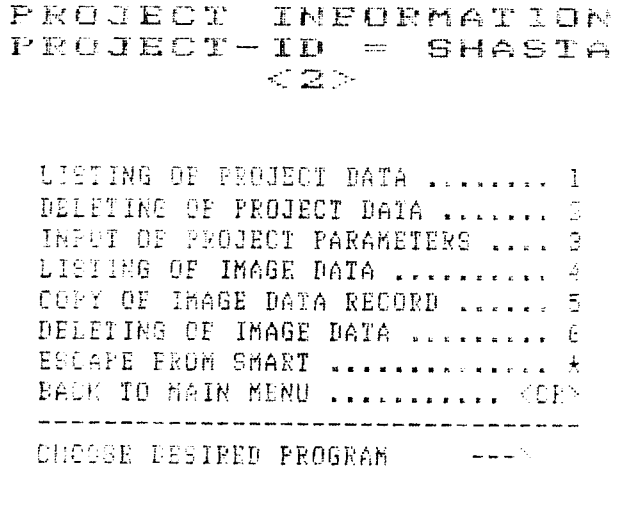

FIGURE 24: Menu of module "PROJECT INFORMATION"

```
GROUND POINT MANAGEMENT
PROJECT - ID = SHASTA
<3>

LIST GROUND CONTROL POINTS ..... 1
INPUT OF GROUND CONTROL POINTS ... 2
READ CONTROL POINTS FROM FILE .... 3
DELETE GROUND CONTROL POINTS ..... 4
CORRECTION OF CONTROL POINTS ..... 5
TRANSFORM CONTROL POINTS ......... 6
ESCAPE ........................... *
BACK TO MAIN MENU ............. <CR>
-----------------------------------
CHOOSE DESIRED PROGRAM        --->
```

FIGURE 25: Menu of module "GROUND POINT MANAGEMENT"

```
ORBIT DATA MANAGEMENT
PROJECT - ID = SHASTA
ORBIT NUMBER =        57
<4>

LIST ORBIT STATIONS ..... 1
INPUT OF ORBIT STATIONS ..... 2
READ ORBIT STATIONS FROM FILE .. 3
DELETE ORBIT STATIONS ..... 4
CORRECTION OF ORBIT STATIONS ... 5
TRANSFORM ORBIT STATIONS ..... 6
COMPUTATION OF ORBIT ..... 7
NEW ORBIT ..... 8
ESCAPE ..... *
BACK TO MAIN MENU ..... <CR>
-----------------------------------
CHOOSE DESIRED PROGRAM     --->
```

FIGURE 26: Menu of module "ORBIT DATA MANAGEMENT"

```
SINGLE RADAR IMAGE:   PROJECT-ID = SHASTA
IMAGE NUMBER =     57          PLATE = UPPER
                  <5>

                  INPUT OF IMAGE PARAMETERS .. 1
                  INNER ORIENTATION ......... 2
                  IMAGE POINT MANAGEMENT ..... 3
                  BUNDLE ADJUSTMENT ......... 4
                  DISTORTION POLYNOMIALS ..... 5
                  PLOTTING ................... 6
                  NEW SINGLE IMAGE ........... 7
                  ESCAPE ..................... *
                  BACK TO MAIN MENU ....... <CR>
                  ----------------------------
                  CHOOSE DESIRED PROGRAM --->
```

FIGURE 27: Menu of module "SINGLE RADAR IMAGE"

```
RADAR STEREO MODEL:   PROJECT-ID = SHASTA
UPPER IMAGE =     57   LOWER IMAGE =     28
                  <6>

                  PROCESSING UPPER IMAGE ..... 1
                  PROCESSING LOWER IMAGE ..... 2
                  IMAGE POINT MANAGEMENT ..... 3
                  BUNDLE ADJUSTMENT .......... 4
                  PLOTTING ................... 5
                  NEW UPPER IMAGE ............ 6
                  NEW LOWER IMAGE ............ 7
                  ESCAPE ..................... *
                  BACK TO MAIN MENU ....... <CR>
                  ----------------------------
                  CHOOSE DESIRED PROGRAM --->
```

FIGURE 28: Menu of module "RADAR STEREO MODEL"

7.4.3 Radar Stereo-Model Set-up

As previously described the radar stereo model set-up in SMART is realized in two steps consisting of the computation of the elements of inner orientation of the radar image pair, followed by an exterior orientation with a radar bundle adjustment.

Inner Orientation: The inner orientation requires the establishment of a relationship between plate or image x, y coordinates and the physical radar measurements of time t and slant range r (see section 2.3). The system uses a so-called 'range reference line' at the near range edge of the image; it would correspond to the start of the sweep on the image recorder. It should be defined by some distinct tick marks (fiducials). In the event that no such marks exist the operator has to create artificial marks and determine the inner orientation in a process of self-calibration together with the exterior orientation.

Exterior Orientation: First of all the measurement of homologue orientation points can be performed like in a comparator by removing manually the x- and y-parallaxes. Second, after a preliminary resection with each image, one is in a nearly parallax-free stereo-model and observation of homologue points is made more convenient. In contrast to analog stereo-photogrammetry the analytical plotter does not need a relative orientation task seperate from absolute orientation. The parameters of relative and absolute orientation are found simultaneously with a so-called bundle adjustment. In our system this approach is the one used for radar images. The basic equations for the radar stereo-adjustment consist of two types:

(a) The squint angle condition :

$$\dot{\underline{s}} \cdot (\underline{p} - \underline{s}) - \sin\tau \; |\dot{\underline{s}}| \cdot |\underline{p} - \underline{s}| = 0 \qquad (16)$$

(b) The range condition :

$$r_s - |\underline{p} - \underline{s}| = 0 \qquad (17.a)$$

for slant range presentations, or

$$(r_g^2 + H^2)^{1/2} - |\underline{p} - \underline{s}| = 0 \qquad (17.b)$$

for ground range presentations.

Each measured point gives rise to two equations of type (16) and (17). In addition each pair of homologue image points produces one additional condition. This is called the co-circularity condition, which defines the location of an imaged point in object space by the intersection of two circles, each defined by two equations of type (16) and (17). The equations are non-linear. Linearized forms are used in an iterative solution.

Observations for the computations are sensor position measurements, image coordinate measurements of ground control points in one or in both images and pairs of homologue image coordinate measurements of stereo model orientation points. Unknowns to be determined within the adjustment are:

- the coefficients of the orbit time polynomials;

- the radar imaging parameters (inner orientation) to convert radar image coordinates to range and time;

- the parameters of a correction polynomial to describe radar image deformations;

- a value for the squint angle;

- unknown object coordinates of homologue orientation points.

The solution for the unknowns in each iteration of the non-linear equation system is obtained in the instruments host processor in a least squares adjustment using the method of conjugated gradients (Schwarz, 1970). This solution method is iterative and may have some advantages for larger equation systems when a small computer must be used and both computing times and storage requirements are limited. Furthermore there is evidence that the method is more robust for this special problem than a strict Gauss solution of normal equations.

Depending on the quality of the approximate values the adjustment process must be repeated iteratively until results satisfy specified termination criteria.

7.4.4 Example Of Radar Stereo Plotting With SIR-A Satellite Data

A Space Shuttle Imaging Radar SIR-A stereo image pair of the Greek islands Cephalonia and Ithaka was used to illustrate the procedure of extracting a digital height model (see Fig. 9). A more detailed study of the stereoscopic computations from such data is presented by Kobrick et al.(submitted). Viewing limitations were discussed by Domik et al.(1983). After model set-up the topographic elevations were digitized in the object coordinate system using profiles and ridge lines; the measurements were entered into the terrain model system GTM. The GTM program enables one to generate contour line plots at chosen interval, to obtain axonometric views of the terrain data and various other products.

Figure 29 shows an axonometric view of the digital elevation model (DEM) of the islands extracted from a map 1 : 200 000, Figure 30 presents the DEM created on the Kern DSR-1 analytical stereo-plotter. A comparison of the two DEM's is possible with the GTM system and reveals that the root mean square differences over all DEM points of the islands amount to $\pm$ 98 meters.

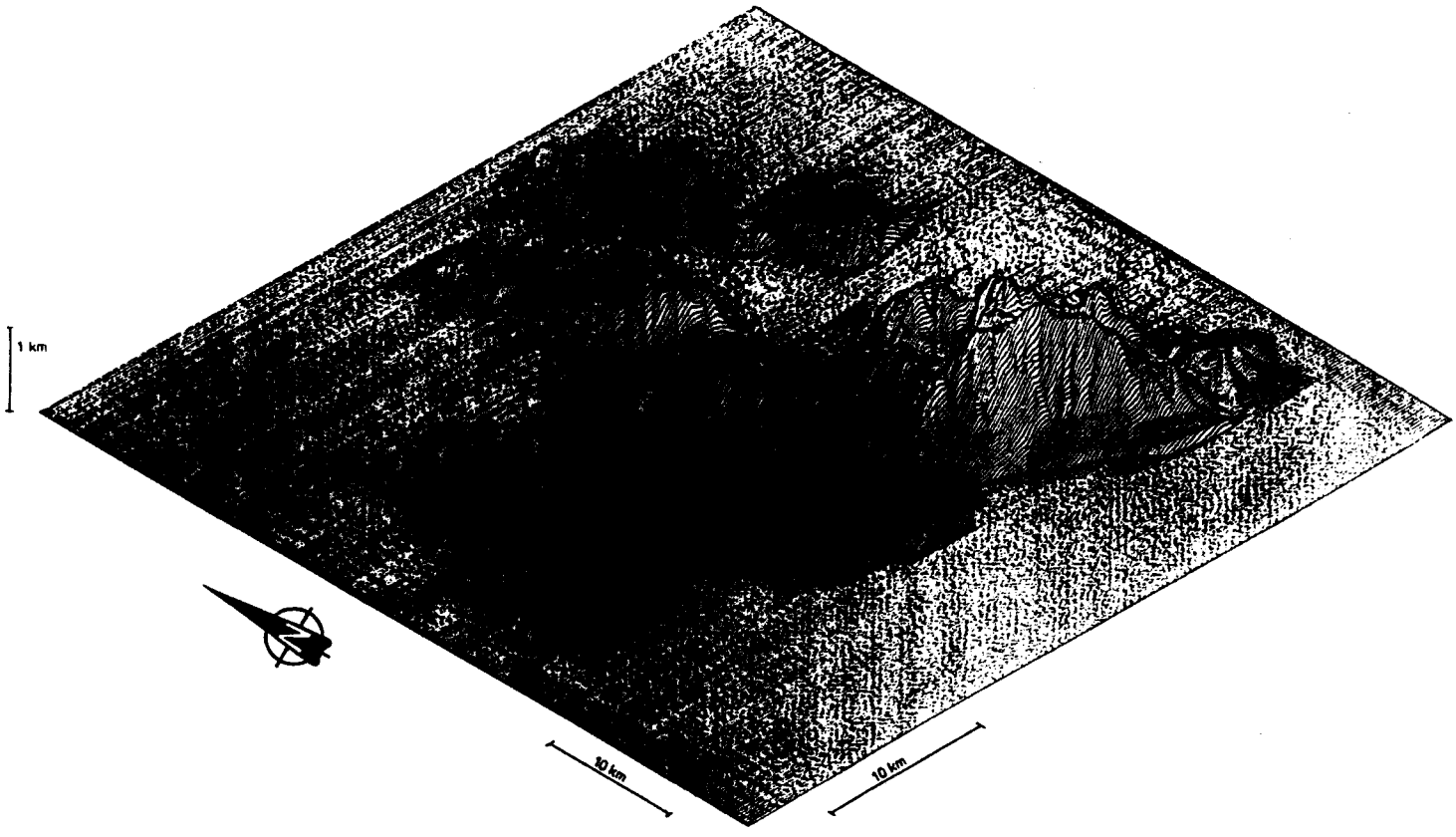

FIGURE 29: Digital elevation model of the Greek islands Cephalonia and Ithaka in axonometric view. Data are extracted from a 1 : 200 000 map, raster interpolation performed by system GTM.

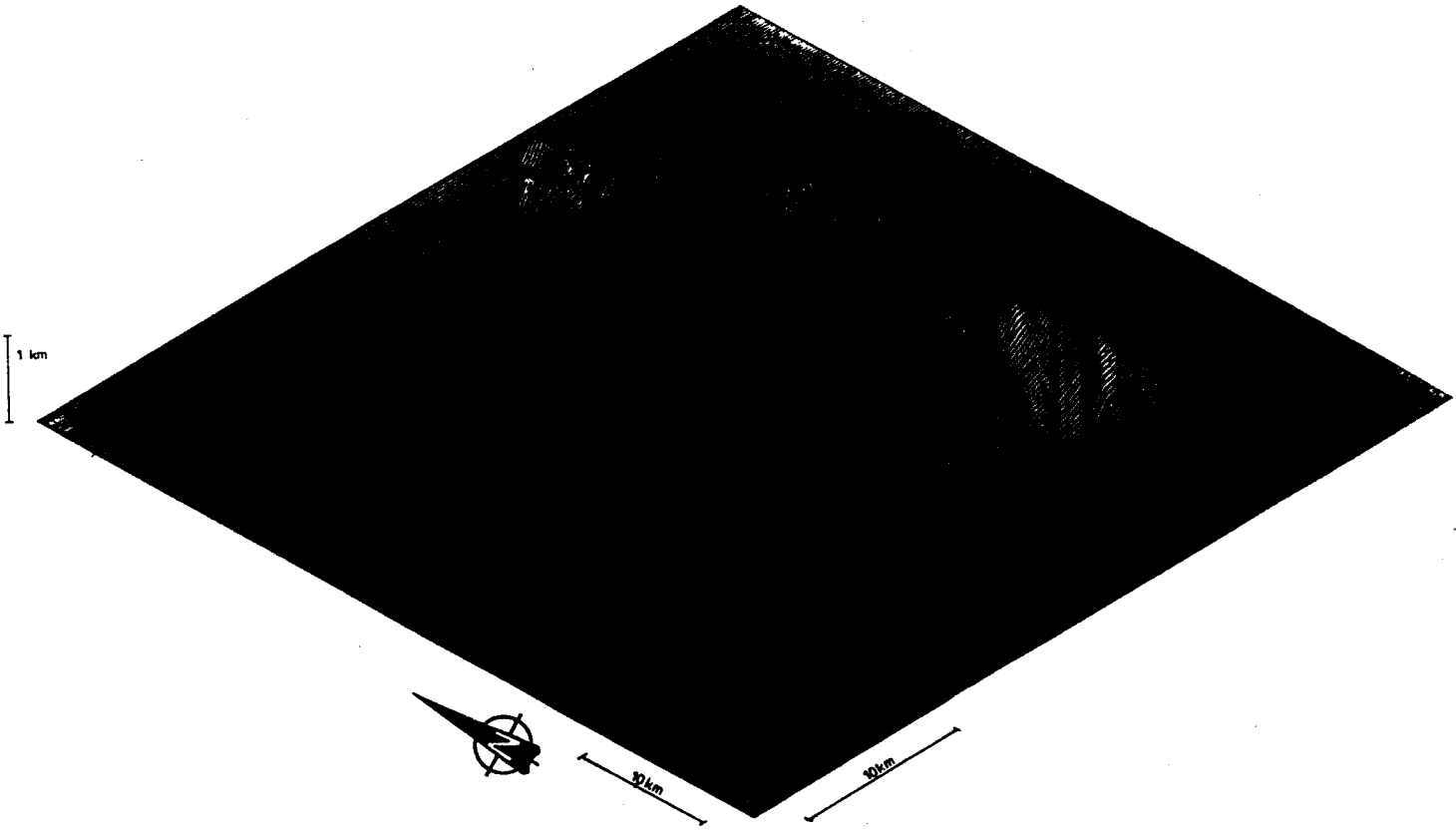

FIGURE 30: Digital elevation model of the Greek islands Cephalonia and Ithaka in axonometric view. Data digitized from SIR-A imagery at a KERN DSR-1 stereo-plotter using the program system SMART.

7.4.5 Software Implementation

The software package is currently installed at a Kern DSR-1 analytical plotter under the name SMART (Stereo Mapping with Radar Techniques).

The DSR-1 standard configuration consists of three independent digital processing units, which are denoted as P1, P2 and P3 (Chapuis, 1980). Processor P1 is the host computer. It serves for development and execution of application programs and performs data transfer between the other processors. The computation of set-up parameters for the radar stereo model is done in P1. Processor P2 receives the radar image orientation parameters from P1 and uses them to convert in real time model coordinates X,Y,Z to radar image coordinates r',t',r",t" and onto DSR-1 plate coordinates x',y' and x",y". P2 also transfers image, model or object coordinates to processor P1 if requested.

Processor P3 is an added convenience for the operator and controls an operator control panel which may be used for communication between operator and DSR-1.

The Kern DSR-1 therefore uses three computers as opposed to other plotters which may employ only one. What seems to be an added complexity in fact is an advantage: the real-time operations are performed by a seperate processor P2 with a clearly defined software interface for a user working with the host P1. The user will therefore work in a familiar, general purpose multi-user environment with an unmodified operating system. The critical real time operations are singled out.

8 RESULTS OF THE INVESTIGATION

8.1 Extraction Of Geologic Information From The Two Shuttle Images

With use of the digital elevation model and parameters from chapter 5, a simulated radar image was created. Real and simulated images are rotated to fit an illumination direction from left (Fig. 31 and Fig. 32).

The correspondence of the radar geometry between the two images is rather accurate. To erase the still existing differences - created by lack of knowledge of the flight path, e.g. flight perturbations, - the real image is registered to the simulation through a relative registration (section 7.2). Approximately 30 homologue points distributed over the image were used as pass points for the process. The error grids (Figure 33 a and b) show good results in the center part but differ much more at the right and bottom edges. This results from the lack of anchor points in these areas, and does not influence the quality of the results.

The geometric rectification was performed on the registered radar images according to section 7.3. The results, denoted as "radar ortho-images" (Fig. 34 and 35) show the use of the two SIR-A images for geological interpretation: Most of the lineaments are enhanced but lithological information cannot be derived from the distribution of the grey values. The effect of slopes in the terrain - strongly backscattering foreslopes versus darker backslopes - controls the shape of the histograms. Removing the slope effect (substracting the effect of the incidence angle from the radar grey values) enhances the thematic two-dimensional surface features in the image. Because SIR-A was not calibrated, and the density values are merely relative digital numbers, only a small number of classes can be distinguished in the processed image. The above-mentioned process is denoted as "radiometric correction".

In Figures 36 and 37 the geometrically and radiometrically corrected images are shown with indication of lithological units. Obviously two classes (G and C) can be distinguished by their level of grey values: While the class of granodiorites shows up in darker tones, the class of Malm carbonates definitely appears lighter.

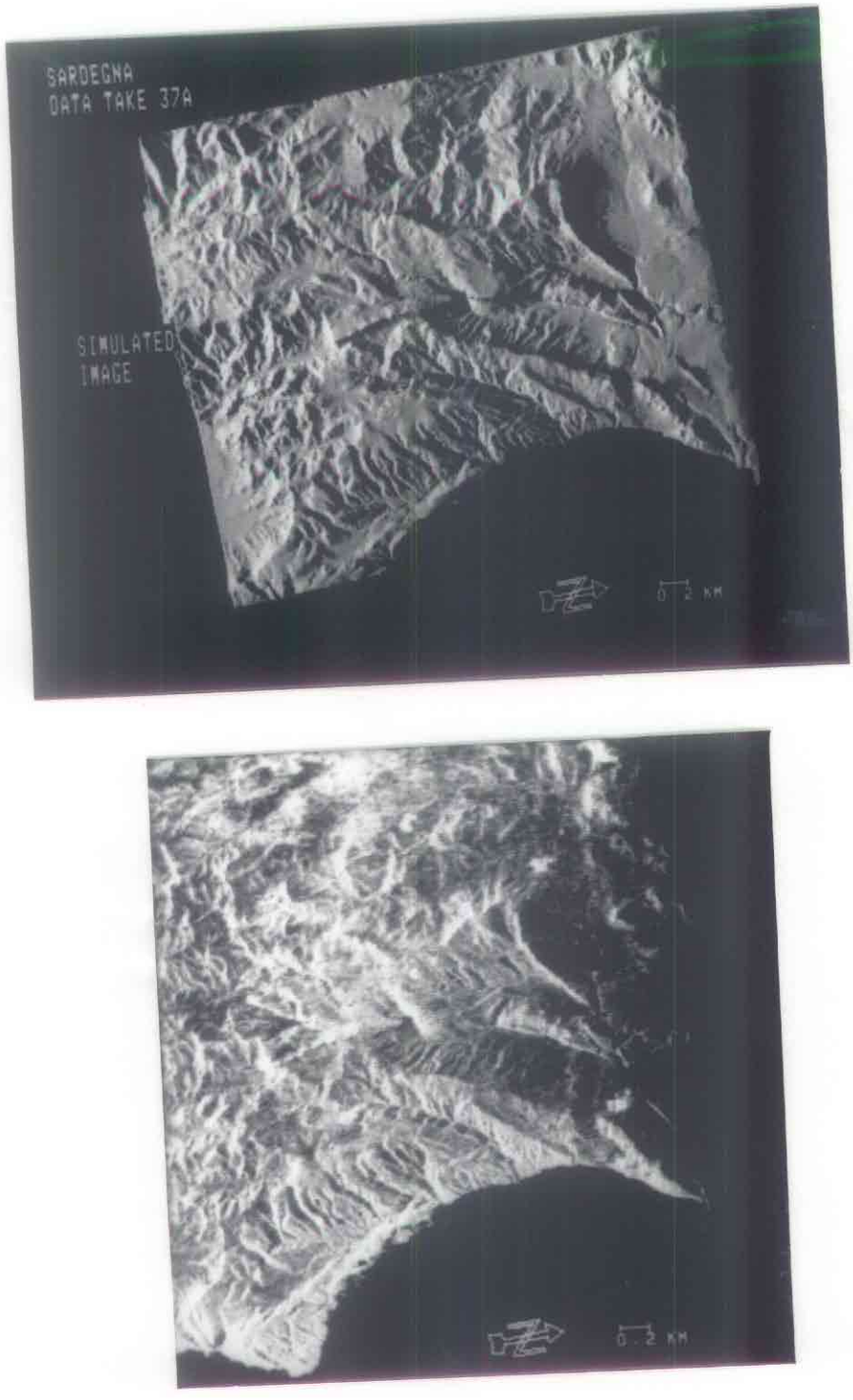

(a)

(b)

FIGURE 31: Comparison of simulated (a) and real radar (b) images for Data Take 37A.

(a)

(b)

FIGURE 32: Comparison of simulated (a) and real radar (b) images for Data Take 35-36.

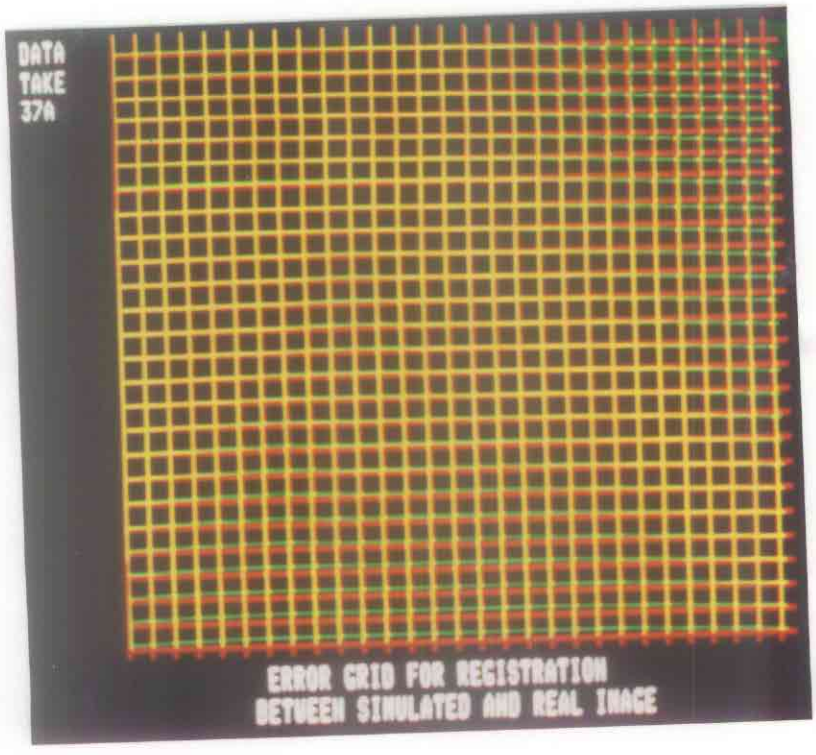

FIGURE 33a: Error grids between real and simulated images for Data Take 37A. Grid in green channel shows distortions.

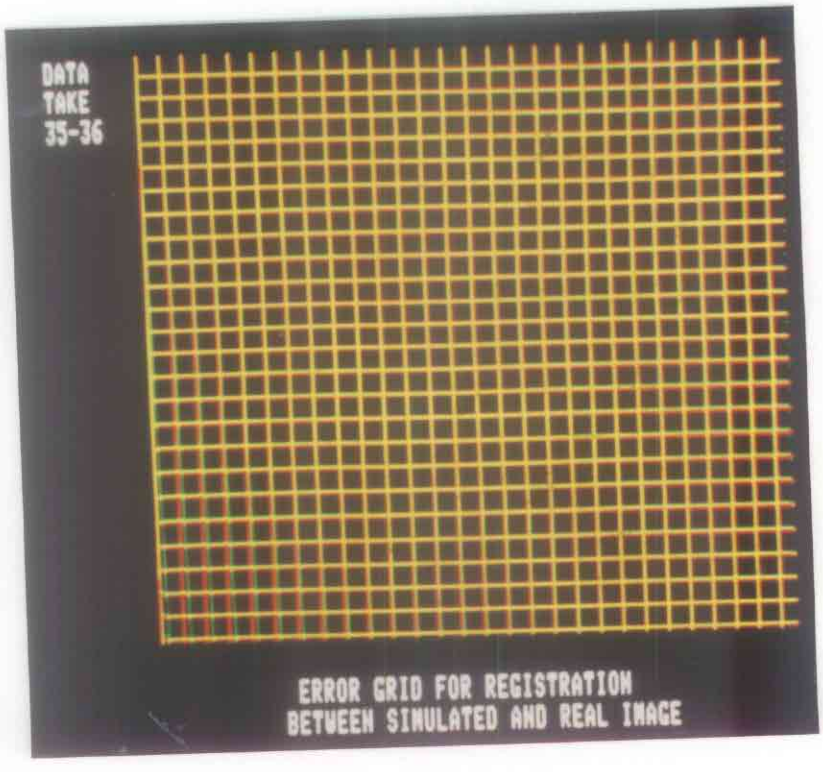

FIGURE 33b: Error grids between real and simulated images for Data Take 35-36. Grid in green channel shows distortions.

FIGURE 34: Radar ortho-image of Data Take 37A.

FIGURE 35: Radar ortho-image of Data Take 35-36.

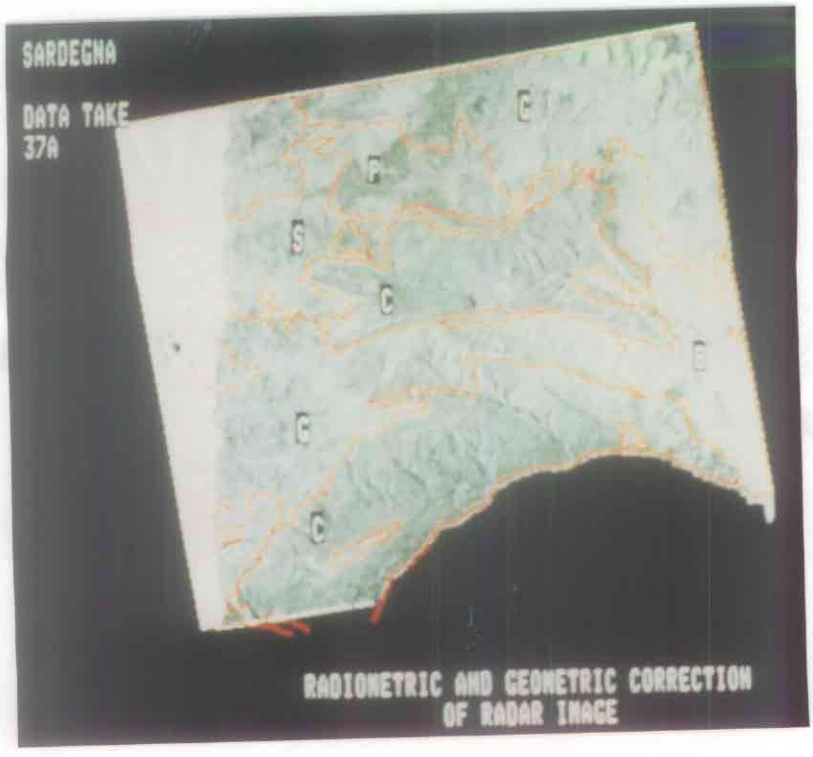

FIGURE 36: Radar image (Data Take 37A) with indication of lithological units after removal of slope effects.

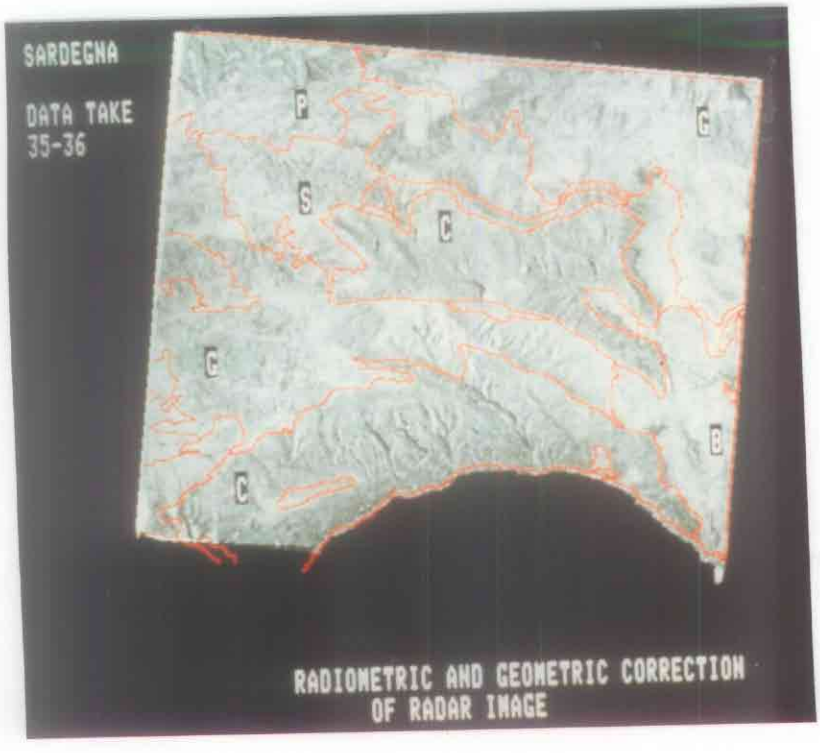

FIGURE 37: Radar image (Data Take 35-36) with indication of lithological units after removal of slope effects.

NOTE:
The process of substracting the grey values reversed the backscattering properties of the two distinguishable classes: The reflectivity of both geological classes lies below the assumed homogeneous reflecting ability, whereas the granodiorites show a higher reflection than the Malm carbonates. Thus the difference between granodiorites and assumed backscatter curve is smaller than the difference between Malm carbonates and the theoretically assumed reflection. Hence the difference image displays lower grey values for the class of granodiorites.

The radiometric correction can be used on either the radar or the radar ortho-image.

8.2 Variation Of The Elevation Angle To Minimize Loss Of Information In Radar Images

The purpose of this radargrammetric investigation was to add new information on the amount of loss one can expect from images with different elevation angles to the already existing knowledge about the requirements of a sensor for geologic applications.

Ten sets of simulated radar images were created with varying elevation angles. The image coordinates were marked for layover, shadow and percentage of foreshortening. The loss of information for the total area was calculated and a comparison made (Table VI). As expected, the high amount of layover and foreshortening with low elevation angles compensates the loss through shadow with high elevation angles. The optimal elevation angle as from the view of radargeometry was 60 degrees to the first data point, yielding an information loss of only 15 percent. For examples of simulated images see Fig. 38 and 39.

It is obvious that other points of views like radiometric aspects have to be considered equally. There should be a differention between the loss of information by radar shadow (no information) and the loss by layover and foreshortening where the structures can still be viewed. For future investigations into this topic weighting of the three regarded parameters as well as consideration of the incident angle are proposed. Even low elevation angles enhance the appearance of structures in the radar images (Bodechtel, 1983).

TABLE VI

EFFECT OF ELEVATION ANGLE ON LAYOVER, FORESHORTENING AND SHADOW

SARDEGNA	Total Area	Relevant Area
%	100	app. 85
km**2	1245	1058.25
Pixel	124500	105825

Elev.Angle (Deg.)	Layover (%)	Foresh. (%)	Shadow (%)	Sum of loss (%)	Sum of loss (km**2)
20	5.03	43.29	0.00	48.32	601.58
30	1.35	35.18	0.06	36.59	455.55
40	0.47	26.36	0.24	27.07	337.02
45	0.12	22.16	0.69	22.95	285.73
50	0.08	18.25	0.97	19.30	240.28
55	0.03	14.65	2.07	16.75	208.54
60	0.01	11.43	3.48	14.92	185.75
65	0.00	8.53	7.82	16.35	203.56
70	0.00	6.10	13.12	19.19	238.92
80	0.00	2.30	35.97	38.27	476.46
45.64 (SIR-A Data Take 35-36)	0.26	22.65	0.30	23.21	288.96
45.57 (SIR-A Data Take 37A)	0.30	22.07	0.24	22.61	281.50
15.45 (Seasat)	9.66	50.24	0.00	59.90	745.76

Flight Altitude for SEASAT: 795 km
other : 260 km

FIGURE 38: Simulated radar image from an altitude of 260 km and elevation angle of 30 degrees to first data point.

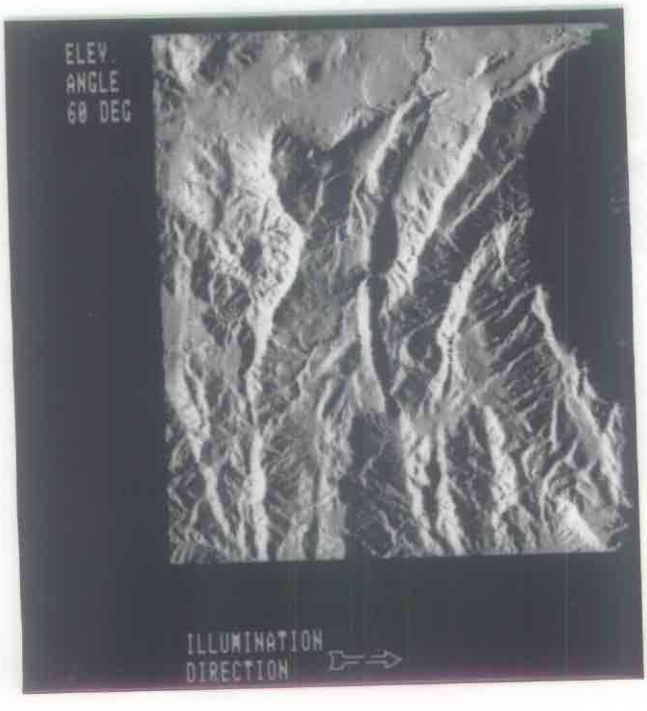

FIGURE 39: Simulated radar image from an altitude of 260 km and elevation angle of 60 degrees to first data point.

8.3 Optimum Parameters For Same-Side Stereo

The above set of simulated images was also used for an investigation in stereo-viewability. Black and white hardcopies of the radar simulations at different look angles and a standard mirror stereoscope were used for evaluation. The image pairs were rated with numbers from 1 to 10, wherby 1 denotes "no stereo-viewability" and 10 denotes "excellent stereo-viewability". The rating was done by a geologist, a photogrammetrist and a specialist in digital radar data processing. Table VII shows the best ranked image pairs of this evaluation:

Table VII

Look angles off nadir (degrees)	Intersection angles (degrees)	Rank order /*/ (1 - 10)
30/55	25	10
20/30	10	9
30/60	30	9
30/50	20	9
20/40	20	8
30/40	10	8
30/45	15	8
40/55	15	8
45/65	20	8

/*/ 1: no stereo-viewability,
10: excellent stereo-viewability

A stereo-pair in anaglyph presentation can be viewed in Fig. 40.

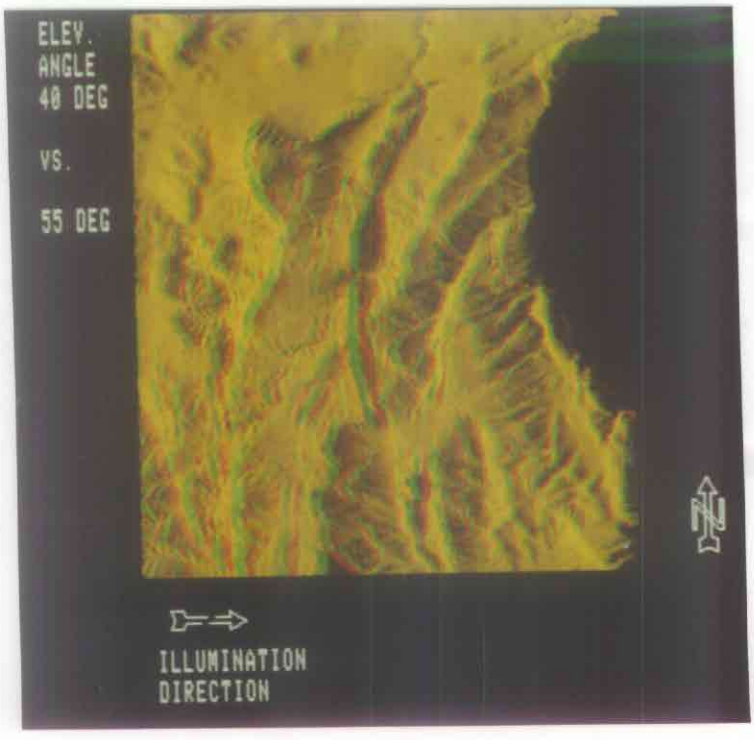

FIGURE 40: Simulated stereo-pair.
NOTE: Green glass for left eye!!!

From Table VII it can be derived, that small intersection angles combined with low elevation angles exaggerate the stereo-impression, whereas the opposite is true for high elevation angles, where the topography appears flat for the viewer.

It is, however, quite obvious, that the present evaluation by only three test persons and the limited number of configurations do not permit sound statements on maximum stereo-impression. For future studies combinations with steps of 5 degrees and some 20 operators are proposed. Also, a ranking from 1 to 5 might be sufficient.

8.4 Variation Of The Flight Path For Enhancement Of Topographic Features In Radar Imagery

As in most cases the illumination effects (and not the radar distortions) cause the enhancement of the features, it is sufficient to create synthetic illuminations instead of synthetic radar images.

Eight different illumination directions in steps of 22.5 degrees were simulated and their effects on the image examined. Even though features normal to the illumination direction are enhanced strongly, they are not lost by viewing them at an angle different from 90 degrees. Linear structures can hardly be viewed when they appear parallel to the illumination direction.

For the limited arrangements investigated (see Table VIII) it can be stated, that - again, only for the studied type of terrain - any two different flight paths are enough to extract all linear geomorphologic features. However, in areas with only subtle changes in relief and/or vaguely expressed lineaments which strike subparallel to the illumination direction, two (simulated) flight paths with only some 20 degrees difference, would certainly be insufficient. More definite statements on that topic would need more intensive investigations with different types of terrain.

Table VIII

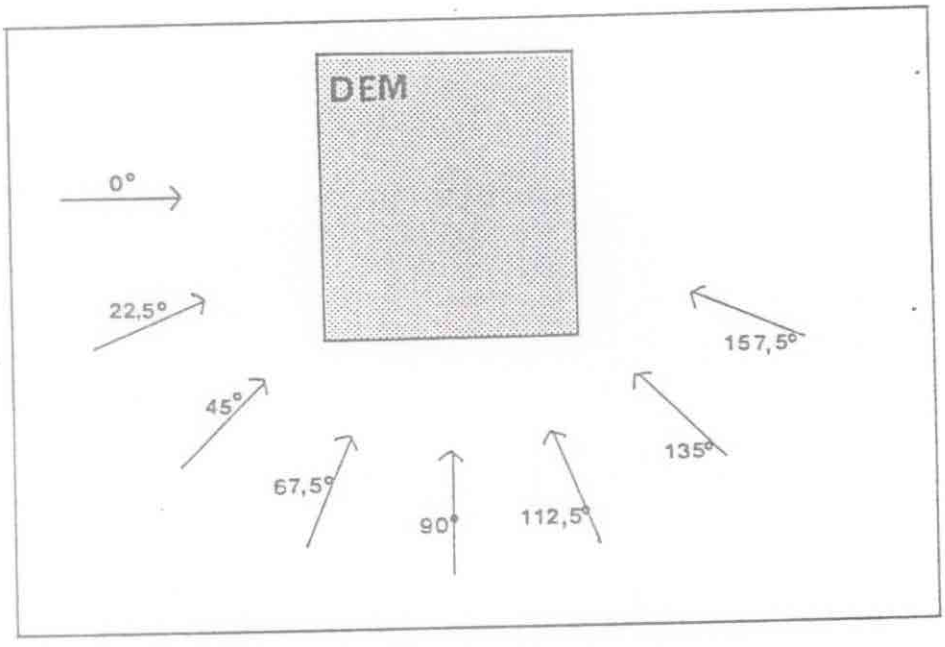

The System parameters at imaging time were chosen as:

Satellite Altitude : 777 km
Elevation angle to
first data point : 20°
Swath width : 80 km

In Fig. 41a and b two simulations (the illumination direction is indicated by arrow) are superimposed on lineament maps. The esteemed reader is kindly asked to focus his attention to the third lineament from left (bottom) which trends N-S. This lineament is not viewable in Fig. 41a, whereas it clearly stands out in Fig. 41b.

FIGURE 41a: Synthetic illumination with lineament map superimposed. Illumination direction 90 degrees (according to Table VIII).

FIGURE 41b: Synthetic illumination with lineament map superimposed. Illumination direction 112.5 degrees (according to Table VIII).

9 CONCLUSIONS

In the first sections of this study it has been shown that a considerable body of work concerning radargrammetry already exists. Most of this concerns analog aircraft imagery. One may argue that a radargrammetric concept is independent of the exact type of data it is applied to. However, satellite imagery can have rather peculiar characteristics: there is very large coverage, potentially rather precise satellite positioning, a very large distance from the object, steep look angles and poor base-to-height stereo-arrangements.

It is in the context of digital satellite image processing, that the theory behind has to be used to develop new concepts, which allow processing of global radar scenes as we will expect from the future ERS-1. As shown in the second part of this report, such processes are existing for:

- geometric rectification of digital radar images for combination radar imagery with data available from other sources or from maps.

- reduction of the effect of incidence angle on the radar image grey values. Thus other target properties (thematic content) are enhanced. This might prove to be of great help when radar images are used for thematic mapping.

- creation of digital elevation models from radar stereo-imagery where topographic data is not available.

The possibilities of a radar image simulator were used to create synthetic terrain scenes with varying imaging and flight parameters. Results show that much higher elevation angles as the ones to be used by ERS-1, would provide optimal image quality as derived from the predicted effects by layover, foreshortening and shadow. Studies on stereo-viewability show that low elevation angles do provide efficient stereo-impression.

The requirement of at least two perpendicular flights to provide efficient data for lineament extraction does not seem to be necessary. It could be shown that, when using ERS-1 imaging parameters (flight altitude and elevation angle), any two imaging sensors with an intersection angle in their flight paths of 22° (at the most), will create radar data, from which all lineaments expressed in topography can be extracted.

10 OUTLOOK

The previous conclusions are limited to the investigations of one test area (Sardegna, Italy). This means that one input parameter - namely the elevation model and its specific properties - was not varied throughout the investigation. This has so be kept in mind when applying the results to other images of different areas.

Consequently, areas with different topographics should be studied in the same manner as proposed in this report, in order to be able to drawn more general conclusions.

Within the scope of this report only SIR-A radar imagery has been used for digital processing and interpretation. Naturally, the amount of information over a certain area will increase if synergistic data sets are available. Thus we propose the combination of digital multi-source remote sensing data sets, as intercalibrated radar imagery from different sensors (e.g. Seasat, SIR-A, SIR-B, SAR-580) and data from sensors other than radar (e.g. Landsat MSS and TM, Metric and Large Format Camera, Moms, Spot).

Additionally available data sets like topographic a thematic information may be integrated.

When working with digital imagery, a first necessary step is digital image processing of single data scene to enhance data quality. The processes to be used differ for various sensor properties and sensor weaknesses as e.g. speckle reduction in radar imagery or destriping of Landsat images.

Current literature on these topics and conventional methods should be reviewed and, if necessary, new methods derived to develop procedures for optimal enhancement of geological information in the individual images.

Another necessary step in the combination of different digital data sets over one area is the availability of a procedure to register the various data layers to one another. This is proposed to be done by the procedure described within this study report, which will register each of the data sets to the geometry of a digital terrain model. The integration of a digital elevation model is necessary, if a certain amount of topographic varyation is present in the area to be studied. For mosaicking different scenes covering the imaged ground portion the conventional approach to register each scene to a reference geometry, e.g. the digital elevation model, is proposed.

Further research and software development in this direction should lead to a computer-assisted geological interpretation system of multiple remote sensing data sets.

11 SELECTED READING

SIMONETT, D.S. and DAVIS R.E., 1983: "Image Analysis-Microwave Region". Manual of Remote Sensing, Chapter 25. American Society of Photogrammetry.

12 BIBLIOGRAPHY

AKOWETZKY W.I. (1968): "On the Transformation of Radar Coordinates into the Geodetic System". Geodezia i Aerofotojomka (in Russian).

AMBROSE W. (1967): "A Radar Image Correlation Viewer". Photogramm. Eng., Vol. 33.

AZEVEDO L. DE (1971): "Radar in the Amazon". Proc. 7th Int. Symp. Remote Sensing of the Environment, Ann Arbor, Michigan.

BAIR G.L. and G.E. CARLSON (1975): "Height Measurement with Stereo Radar". Photogramm. Eng. and Remote Sensing Vol. 41.

BAIR G.L. and G.E. CARLSON (1974): "Performance Comparison of Techniques for Obtaining Stereo Radar Images". IEEE Trans. on Geoscience Electronics, GE-11.

BAKER J., E.M. MIKHAIL (1975): "Geometric Analysis and Restitution of Digital Multispectral Scanner Data Arrays". LARS Information Note 05 28 75, Purdue Univ., USA.

BERLIN L.G. and G.E. CARLSON (1974): " Radar Mosaics". The Professional Geographer, Vol. 23, No. 1.

BICKNELL T. et al. (1975): " A Study of Determine the Feasibility of Using Radar Techniques for Public Land Surveying". Jet Propulsion Laboratory Report under Contract to the Bureau of Land Management, Contract No. 5300-PH-995, Pasadena, California.

BLOM R.G. and M. DAILY (1982): "Radar Image Processing for Rock-Type Discrimination"; IEEE Transactions on Geoscience and Remote Sensing, Vol. GE-20, No. 3, pp. 343 - 351.

BODECHTEL J. (1983): "Requirements for Spaceborne Remote Sensing in Geology". Proc. Alpbach Summer School Sept. 1983, ESA Spec. Publ. 205, Paris.

BOSMAN E. et al. (1971): " Project Karaka - The Transformation of Points from Side Looking Radar Images into the Map System". Final Report, Part 1, Netherlands Interdepartmental Working Community for the Application and Research of Remote Sensing Techniques (NIWARS), Delft.

BOSMAN E.R., E. CLERICI, D. ECKHART, K. KUBIK (undated): "Project BEBLOKA - The Transformation of Points from Overlapping Images Obtained with Different Sensors into the Map System". Final Report, Netherlands Interdepartmental Working Community for the Application a.Research of Remote Sensing Techniques (NIRWARS), Delft.

BOSMAN E.R., E. CLERICI, D. ECKHART, K. KUBIK (1972): "Information of Points from Side-Looking-Radar Images into the Map System". Bildmessung und Luftbildwesen, Vol. 42, No. 2.

BOSMAN E.R., E. CLERICI, D. ECKHART, K. KUBIK (1972): "KARIN-A Program system for the Mapping of Remote Sensing Information". Pres. Paper, 12th Congress, Int.Soc. Photogrammetry, Ottawa, Canada; and Final Report, Netherlands, Interdepartmental Working Community for the Application a.Research of Remote Sensing Techniques (NIRWARS), Delft.

BROWN W. et al. (1981): "Application of Seasat SAR Digitally Correlated Imagery for Sea Ice Dynamics". Invited Paper, 1981 AGU-Meeting, Baltimore, USA.

BRYAN M.L., W. STROMBERG, T. FARR (1977): "Computer Processing of SAR L-band Imagery". Photogramm. Eng. and Remote Sensing, Vol. 43, No. 10, pp 1283 - 1294.

CARLSON G.E. (1973): "An Improved Single Flight Technique for Radar Stereo". IEEE Trans.on Geoscience Electronics, GE-11, No. 4.

CHAPUIS A. (1980): "Das Kern System DSR-1/GP-1. Analytisches Stereo-Auswertegeraet und graphisches Peripheriegeraet". 14th ISP Congress, Commission II, Hamburg 1980.

CIMINO J., ELACHI C. (1982): "SIR-A Radar Parameters. On/Off Times. Latitude and Longitude". Internal JPL-Report Pasadena, Cal. 91109, USA.

CLAVELOUX B.A. (1960): "Sketching Projector for Side Looking Radar Photography". Photogramm. Eng., Vol. 26.

CRANDALL C.J. (1963): "Advanced Radar Map Compilation Equipment". Photogramm. Eng., Vol. 29.

CRANDALL C.J. (1969): "Radar Mapping in Panama". Photogramm. Eng., Vol. 35.

CURLANDER J. (1981a): "Geometric and Radiometric Distortion in Spaceborne SAR Imagery". Invited Paper, NASA Workshop of Registration - Rectification for Terrestrial Applications. November 17 - 19. Jet Propulsion Lab., Pasadena, USA.

CURLANDER J. (1981): "Sensor to Target Range Determination". IPL-Interoffice Memorandum 334. 7-80-056. Jet Propulsion Laboratory, Pasadena, USA.

DAILY M. et al.(1978): "Application of Multispectral Radar a. Landsat Imagery of Gelogic Mapping in Death Vally". JPL-Publication, 78-19, Pasadena, USA, 47 pp.

DALKE G. et al. (1968): "Regional Slopes with Non Stereo Radar". Photogramm. Eng., Vol. 24.

DBA SYSTEMS (1974): "Research Studies and Investigations for Radar Control Extensions". DBA Systems, Inc., P.O. Drawer 550, Melbourne, Florida, Defense Documentation Center Report No. 530784L.

DELLWIG L.F. (1980): "A New Look at Togo through the Eyes of a SLAR". In Radar Geology, An Assessment, JPL-Publication 80 - 61, Jet Propulsion Laboratory, Pasadena, USA.

DERENYI E.E. (1970): "An Exploratory Investigation into the Relative Orientation of Continuous Strip Imagery". Ph.D. Thesis and Research Report No. 8, Univ. of New Brunswick, Canada.

DERENYI E.E. (1972): "Geometric Consideration in Remote Sensing". Proc. First Canadian Symp. on Remote Sensing, Ottawa.

DERENYI E.E. (1974): "SLAR Geometric Test". Photogramm. Eng., Vol. 40.

DERENYI E.E. (1974): "Metric Evaluation of Radar and Infrared Imageries". Second Canadian Symp. on Remote Sensing, Univ. of Guelph, Guelph, Ontario.

DERENYI E.E. (1975): "Topographic Accuracy of Side Looking Radar Imagery". Bildmessung und Luftbildwesen, 1975, No. 1.

DERENYI E.E. (1975): "Terrain Heights from SLAR Imagery". Pres.at the 41st Annual Conv. Am. Soc. Photogramm., Washington, D.C., March.

DIARRA G. (1982): "A Digital Image Rectification System Description and Examples", DIBAG Report Nr. 10, Graz Research Center, Austria.

DICARLO C. et al. (1968): "All Weather Mapping". Presented Paper, International Congress of Surveyors (FIG), London, England.

DICARLO C. et al. (1971): "DoD Data Processing Equipment for Radar Imagery". Pres. Paper, Int. Congress of Surveyors, Wiesbaden.

DOMIK G., F. LEBERL, J. RAGGAM (1983): "Evaluation of Radargrammetric Stereo". DIBAG Report Nr. 11, Graz Research Center. 127 p.

DOMIK G., M. KOBRICK, F. LEBERL (1984): "Analyse von Radarbildern mittels digitaler Hoehenmodelle". Bildmessung und Luftbildwesen.

DOWIDEIT G. (1975): "A Simulation System for Theoretical Analysis of Radar Restitution and a Test by Adjustment". Proc. Symp. Comm.III, Int. Soc. Photogramm., Stuttgart, W. Germany, in Deutsche Geodaetische Kommission, Reihe B., Heft No. 214.

DOWIDEIT G. (1977): "Eine Blockausgleichung fuer Abbildungen des seitwaertschauenden Radar (SLAR)". Wissensch. Arbeiten der Lehrstuehle fuer Geodaesie etc., Nr. 75, Technische Universitaet Hannover, FRG, 185 pp.

DOWIDEIT G. (1977): "Eine Blockausgleichung fuer Aufzeichnungen des Seitwaerts-Radar (SLAR)". Bildmessung und Luftbildwesen Vol. 45, No. 1, pp 17 - 23.

EBNER H., R. HOESSLER (1978): "The Use of Gauss-Markov Processes in Digital Rectification of Remote Sensing Data". Proceedings of the LSP-Comm., 3. Symposium, Moscow, pp. 258 - 265.

EGBERT E. (1969): "Calculation of Ground Street Lenghts and Area from Radar Measurements". Simonnett, D.S., (ed.), "The Utility of Radar and Other Remote Sensors in Thematic Land Use Mapping from Spacecraft". Annual Report, U.S. Geolog. Survey Interagency Report-NASA 140.

ESA (1981): "ERS-1 Announcement of Opportunity for Participation in the Proposed ERS-1 Mission". APP (81) 1, Part B.

ESTEN R.D. (1953): "Radar Relief Displacement and Radar Parallax". USAERDL Report No. 1294, Fort Belvoir, Virginia.

FIORE C. (1967): "Side Looking Radar Restitution". Photogramm. Eng., Vol. 33.

FORD J. (1982): "Resolution Versus Speckle Relative to Geologic Interpretability of Spaceborne Radar Images". IEEE Transactions on Geoscience and Remote Sensing, Vol. GE-20, No. 4, pp. 434-444.

FORD J., J.B. CIMINO, Ch. ELACHI (1983): "Space Shuttle Columbia Views the World with Imaging Radar: the SIR-A Experiment". JPL-Publication 82 - 95. Pasadena, California.

FROIDEVAUX C.M. (1980): "Radar, an Optimum Remote Sensing Tool for detailed Plate Tectonic Analysis and its Application to Hydrocarbon Exploration". (An Example in Irian Jaya, Indonesia). In Radar Geology, An Assessment, JPL-Publication 80 - 61, Jet Propulsion Laboratory, Pasadena, USA.

FROST V.S., M.S. PERRY, L.F. DELLWIG, I.C. HOLTZMAN (1983): "Digital Enhancement of SAR Imagery as an aid in Geologic Data Extraction". Photogramm. Eng. and Remote Sensing, Vol. 49, No. 3, pp. 357 - 364.

FROST V.S., K.S. SHANMUGAN, T.C. HOLTZMAN (1984): "The Influence of Sensor and Flight Parameters on Texture in Radar Images". IEEE Transactions on Geoscience and Remote Sensing, Vol. GE-22, No.5, pp. 440-448.

GEIER F. (1971): "Beitrag zur Geometrie des Radarbildes". Ph.D. Thesis, Techn. Univ., Graz.

GEIER F. (1972): "Fundamentals of Orientation for Radar PPI Images with approximated Horizontal Distances". Pres. Paper, 12th Congress, Int. Soc. Photogramm., Ottawa, Canada.

GLUSHKOV W.M. et al. (1972): "Toros-Side Looking Radar Systems and its Application for Sea Ice Condition Study and for Geologic Explorations". Pres. Paper, 12th Congress, Int.Soc.Photogramm., Ottawa, Canada.

GOODYEAR (1972): "Flight Test Report All-Weather Topographic Mapping System AN/ASQ-142". Contract No.F 33657-70-0769, Goodyear Aerospace Corp., Lichtfield Park, Arizona.

GOODYEAR (1974): "Preliminary Imagery Data Analysis Goodyear Electronic Mapping System (GEMS)". Goodyear Aerospace Corp., Report GIB-9342, Code 99696.

GRACIE G. et al.(1970): "Stereo Radar Analysis". US Engineer Topographic Laboratory, Fort Belvoir, Virginia, Report No. FTR-1339-1.

GRACIE G. and E. D. SEWELL (1972): "The Metric Quality of Stereo Radar". Proc.of the Techn. Program, Electro-Optical Systems Design Conference, New York.

GRAHAM L.C. (1970): "Cartographic Applications of Synthetic Aperture Radar". Proc. Am. Soc. Phctogramm., 37th annual Meeting; and Goodyear Aerospace Corp., Report GERA-1626.

GRAHAM L.C. (1972): "An Improved Orthographic Radar Restitutor". Presented Paper, 12th Congress, Int. Soc. Photogramm., Ottawa, Canada, a. Goodyear Aerospace Corp., Report GERA-1831.

GRAHAM L.C. and H.O. RYDSTROM (1974): "Synthetic Aperture Radar Applications to Earth Resources Development". Goodyear Aerospace Corp., Report GERA-2010, Code 99696.

GRAHAM L.C. (1975): "Geometric Problems in Side-Looking Radar Imaging". Proc. Symp. Comm. III. Int. Soc. Photogramm.; Stuttgart, W. Germany, in Deutsche Geodaetische Kommission, Reihe B, Heft No. 214.

GRAHAM L.C.(1975): "Flight Planning for Stereo Radar Mapping". Proc.Am. Soc. Photogramm., 41st Meeting, Washington, D.C.

GRAHAM L.C. (1976): "Earth Resources Radar Stereo Considerations". Goodyear Aerospace Corp., Arizona Division, AEEM-550, 13 p.

GREVE C. and W. COONEY (1974): "The Digital Rectification of Side Looking Radar". Proc. Am. Soc. Photogramm., Annual Convention, Wash., C.D.

GUERTIN F., E. SHAW (1981): "Definition and Potential of Geocoded Satellite Imagery Products". 7th Canadian Symp. on Remote Sensing, Winnipeg, Manitoba.

HAGFORS T. (1964): "Backscattering from an Undulating Surface with Applications to Radar Returns from the Moon", J. Geophys. Res. 1969, pp.3779-3784

HARRIS H. M. (1981): "Mission Operations Procedure Handbook", JPL Publication 750-172, pp. 10-72, Jet Propulsion Laboratory, Pasadena.

HIRSCH TH. and J. VAN KUILENBURG (1976): "Preliminary Tests of the EMI-SLAR Mapping Quality". Netherlands Interdepartmental Working Community for the Appli. a.Res. of Remote Sensing (NIWARS), Internal Report No. 39, Delft.

HOCKEBORN H.A. (1971): "Extraction of Positional Information from Side Looking Radar". Bildmessung und Luftbildwesen, Vol. 39, No. 1.

HOFFMANN P. (1958): "Photogrammetric Applications of Radar Scope Photographs". Photogramm. Eng., Vol. XXIV.

HOHENBERG F. (1950): "Zur Geometrie des Funkmessbildes". Austrian Academy of Sciences, Math.-Naturwissenschaftliche Klasse, Vienna, Vol. 2-3.

HOLTZMAN I.C. et al. (1977): "Radar Image Simulation: Validitation of the Point Scattering Method". Report ETL-0017 (Vol.1), USA Engineer Topographic Laboratory, Fort Belvoir, USA.

IEEE-CONFERENCE (1981): "IGARSS 81". Intern. Geoscience and Remote Sensing Symposium, Washington D.C., IEEE Catalog No. 81 CH 1656-8.

IEEE-CONFERENCE (1983): "IGARSS 83". Intern. Geoscience and Remote Sensing Symposium, San Francisco.

INNES R.B. (1964): "Principles of SLAR Measurement of the Third Coordinate of Target Position". Report of Project Michigan No. 2900-474-T.

ITO N. (1981): "SAR Digital Processing System". Presented Paper ISPRS-SAR Working Group II 15, Frascati, Hobs.

JASKOLLA F., H. KAUFMANN (1984): "The applicability of Improved Remote Sensing Data for Lothological and structural Mapping". Proc. of IGARSS 1984 Symposium, Strasbourg.

JENSEN H. (1972): "Mapping with Coherent-Radiation Focused Synthetic Aperture Side-Looking Radar". In "Operational Remote Sensing: An Interactive Seminar to Evaluate Current Capabilities". Am.Soc. Photogramm.

JENSEN H. (1975): "Deformations of SLAR Imagery-Results from actual Surveys". Proc. Symp. Comm. III, Int. Soc. Photogramm., Stuttgart, W.Germany, in Deutsche Geodaetische Kommission, Reihe B, Heft No. 214.

KAUPP V.H., W.P. WAITE, H.C. MACDONALD (1982): "Indicence Angle Considerations for Spacecraft Imaging Radar". IEEE Transactions on Geoscience and Remote Sensing, Vol. GE-20, No. 3, pp. 384 - 390.

KAUPP V.H. et al.(1982): "Comparison of Simulated Stereo Radar Imagery. IGARSS'82, Munich, Paper TA4, June 1 - 4.

KOBER C.L. et al.(1950): "Determination of Target Height from Radar PPI-Photographs". Air Force Techn. Report No. 6500, Wright Air Development Center, Ohio.

KOBRICK M., F. LEBERL, J. RAGGAM (in print): "Convergent Stereo with Shuttle Imaging Radar". Jet Propulsion Laboratory, M.S. 183 - 701, Pasadena, California.

KONECNY G. and E.E. DERENYI (1966): "Geometric Consideration for Mapping from Scan Imagery". Proc. 4th Symposium Remote Sensing of the Environment. Ann Arbor, Michigan.

KONECNY G. (1970): "Metric Problems in Remote Sensing". Publications of the International Inst. for Aerial Survey and Earth Sciences (ITC), Series A, No. 50, Delft.

KONECNY G. (1971): "Orientierungsfragen bei Streifenbildern und Aufnahmen der Infrarotabtastung". Bildmessung und Luftbildwesen, Vol. 41, No. 1.

KONECNY G. (1972): "Geometrical Aspects of Remote Sensing". Arch. Int. Soc. Photogramm., Invited Paper, 12th Congress, Ottawa, Canada.

KONECNY G. (1972): "Geometrische Probleme der Fernerkundung". Bildmessung und Luftbildwesen, Vol. 42, No. 2.

KONECNY G. (1975): "Approach and Status of Geometric Restitution for Remote Sensing Imagery". Pro. Symp. Comm. III, Int. Soc. Photogramm., Stuttgart, W. Germany, in Deutsche Geodaetische Kommission, Reihe B, Heft No. 214.

KOOPMANS B. (1974): "Should Stereo SLAR Imagery be Preferred to Single Strip Imagery for Thematic Mapping?". ITC-Journal 1974-3, Enschede.

KOOPMANS B. (1974): "Drainage Analysis on Radar Images". ITC-Journal, 1973-3, Enschede.

KORNEEV IU. N. (197-): "Analytical Method for Photogrammetric Processing of a Single Radar Photograph". Geodezia i Aerofotosjomka, No. 2, Moskow.

KRATKY V. (1979): "SEASAT Orbit Effects on Imaging Geometry of Synthetic Aperture Radar". 3rd GDTA Symposium, Toulouse.

LA PRADE G.L. (1963): "An Analytical and Experimental Study of Stereo for Radar". Photogramm. Eng., Vol. 29.

LA PRADE G.L. (1969): "Elevations from Radar Imagery". Photogramm. Eng., Vol. 35.

LA PRADE G.L. (1970): "Subjective Considerations for Stereo Radar". Goodyear Aerospace Corp., Report GIB-9169, and Photogramm. Eng.

LA PRADE G.L. (1972): "Stereoscopy - A More General Theory". Photogramm. Eng., Vol. 38, pp. 1177 - 1187.

LA PRADE G.L. (1973): "Stereoscopy - Will Facts of Dogma Prevail?". Photogramm. Eng., Vol. 39, pp. 1271 - 1275.

LA PRADE G.L. (1973): "A More General Theory of Stereoscopy". Goodyear Aerospace Corp., Arizona Division, Litchfield Park, GIB-9268, Rev. A, 58 p.

LA PRADE G.L. (1975): Addendum to GiB-9169, "Subjective Considerations for Stereo Radar". Goodyear Aerospace Corp., Arizona Division, Litchfield Park.

LA PRADE G.L.(1975): "Stereoscopy". Goodyear Aerospace Corp., Arizona Division, Litchfield Park, GERA-2120, Code 99696; 57 p.

LA PRADE G.L. (1975): "Radar Signature of Inverted Catenary with Equilateral Triangular Cross Section (St. Louis Gateway Arch)". Arizona Electronics Eng. Memo. No. 525, Goodyear Aerospace Corp., Arizona Div., Litchfield Park, Arizona.

LA PRADE G.L. et al. (1980): "Stereoscopy". Chapter X, Manual of Photogrammetry, 4th Edition.

LEBERL F. (1970): "Metric Properties of Imagery Produced by Side Looking Airborne Radar and Infrared Line Scan Systems". Publications of the International Inst. for Aerial Survey and Earth Sciences (ITC), Series A, No. 50, Delft.

LEBERL F. (1971): "Vorschlaege zur instrumentellen Entzerrung von Abbildungen mit Seitwaerts Radar (SLAR) und Infrarotabtastsystemen". Bildmessung und Luftbildwesen, Vol. 39.

LEBERL F. (1971): "Remote Sensing - Neue Methoden zur Wahrnehmung auf Abstand". Oesterreichische Zeitschrift fuer Vermessungswesen, No. 6.

LEBERL F. (1971): "Untersuchungen ueber die Geometrie und Einzelbildauswertung von Radarschraegaufnahmen". Diss., Techn. Univ., Wien.

LEBERL F. (1972): "On Model Formation with Remote Sensing Imagery". Oesterr. Zeitschrift fuer Vermessungswesen, Vol. 60, pp. 93 - 61.

LEBERL F. (1972): "Evaluation of Single Strips of Side Looking Radar Imagery". Arch. Int.Soc.Photogramm., Invited Paper, 12th Congress, Ottawa, Canada.

LEBERL F. (1972): "On Model Formation with Remote Sensing Imagery". Oesterr. Zeitschrift fuer Vermessungswesen und Photogrammetrie, No. 2.

LEBERL F. (1972): "Radargrammetria para los Interpretes de Imagenes". Centro Interamericano de Fotointerpretacion, (CIAF), Bogota, Colombia.

LEBERL F. (1974): "Evaluation of SLAR Image Quality and Geometry for PRODRADAM". ITC-Journal, Vol. 2, No. 4, Enschede.

LEBERL F. (1975): "The Geometry of, a. Plotting from, Single Strips of Side Looking Airborne Radar Imagery". Int. Institute for Aerial Survey and Earth Sciences (ITC), Techn. Report No. 1, Enschede.

LEBERL F. (1975): "Radargrammetry for Image Interpreters". Int. Institute for Aerial Survey and Earth Sciences (ITC), Techn. Report No. 2, Enschede.

LEBERL F. (1975): "Radargrammetric Point Determination PRORADAN". Bildmessung und Luftbildwesen, Vol.45, No. 1.

LEBERL F. (1975): "Sequential and Simultaneous SLAR Block Adjustment". Photogrammetria, Vol. 31, No. 1.

LEBERL F. (1975): "Lunar Radargrammetry with ALSE-VHF Imagery". Proc. Am. Soc. Photogramm., Fall Tech. Meeting, Phoenix, Arizona.

LEBERL F., T. FARR, L. BRYAN, C. ELACHI (1976): "Study of Arctic Sea Ice Drift from L-Band Side Looking Radar Imagery". Proc. Am. Soc. Photogramm., 42nd Annual Conv., Washington, D.C.

LEBERL F. (1976): "Mapping of Lunar Surface from Side Looking Orbital Radar Images". The Moon, Vol. 15, No. 3/4.

LEBERL F. (1976): "Imaging Radar Applications to Mapping and Charting". Photogrammetria, Vol. 32.

LEBERL F., J. JENSEN and J. KAPLAN (1976): "Side-Looking Radar Mosaicking Experiment". Photogramm. Eng. and Remote Sensing, Vol. 42.

LEBERL F. (1977): "Radar Mapping Applications using Single Images, Stereo Pairs, and Image Blocks: Methods and Applications". Revista Brasileira de Cartographia, No. 20.

LEBERL F., C. ELACHI (1977): "Mapping with Satellite Side-Looking Radar". Proceedings, 2nd GDTA Symposium, St. Mande, France.

LEBERL F. (1978): "Satellitenradargrammetrie". Deutsche Geodaetische Kommission, Series C, No. 239, Munich, 156p.

LEBERL F. (1978): "Current Status and Perspectives of Active Microwave Imaging for Geoscience Application". ITC Journal, 1978, 1.

LEBERL F., H. FUCHS (1978): "Photogrammetric Differential Rectification of Radar Images". Pres. Paper Symp. of Comm. III of the Intl. Soc. Photogrammetry, Moscow.

LEBERL F., H. FUCHS (1978): "Photogrammetric Differential Rectification of Radar Images". Mittl. d. Geod. Inst. No. 33, TU-Graz, 8010 Graz, Austria.

LEBERL F. et al. (1979): "Mapping of Sea-ice and Measurement of its Drifts Using Aircraft Synthetic Aperture Radar Images". J. Geophysical Research, Vol. 84, No. C4.

LEBERL F. (1979): "Accuracy Aspects of Stereo-Side-Looking Radar". JPL-Publication 1979 - 17, Jet Propulsion Lab., Pasadena, USA

LEBERL F. (1980): "Preliminary Radargrammetric Assessment of SEASAT-SAR Images". Mitteilungen der geodaetischen Institute, No. 33, Tech. Univ., Graz.

LEBERL F., E. CLERICI (1980): "Current Status of Metric Reduction of Active Sensor Data". Archives of the Intl. Soc. of Photogrammetry, Vol. 23/B.3, pp. 435-450.

LEBERL F. (1981): "The Venus Orbital Imaging Radar, (VOIR) Mission". Proceedings, Alpbach summer School, 1981, ESA Spec. Publ. 205, Paris.

LEBERL F., J. RAGGAM, C. ELACHI, W. CAMPBELL (1981): "Measuring Sea Ice Motion from Seasat SAR Images". Invited Paper, 1981 AGU-Meeting, Baltimore, USA. Submitted to Journal of Geophysical Research.

LEBERL F., H. FUCHS, J. FORD (1981): "A Radar Image Time Series". International Journal of Remote Sensing, Vol. 2, No. 2.

LEBERL F. (1983): "Photogrammetric Aspects of Remote Sensing with Imaging Radar". Remote Sensing Reviews, Harwood Academic Publishers, London. pp. 71 - 158.

LEBERL F., J. RAGGAM, M. KOBRICK (1985): "Stereo Viewing of Radar Images". IEEE Trans. on Geoscience and Remote Sensing.

LEONARDO E. (1959): "An Application of Photogrammetry to Radar Research". Photogramm. Eng., Vol. 25.

LEONARDO E. (1963): "Comparison of Imaging Geometry for Radar and Photographs". Photogramm. Eng., Vol. 39.

LEONARDO E. (1964): "Capabilities and Limitations of Remote Sensors". Photogramm. Eng., Vol. 30.

LEVINE D. (1960): "Radargrammetry". Mac Graw-Hill Book Company, New York.

LEVINE D. (1963): "Principles of Stereoscopic Instrumentation for PPI-Photographs". Photogramm. Eng., Vol. 30.

LEVINE D. (1965): "Automatic Production of Contour Maps from Radar Interferometric Data". Pres. Paper, Fall Tech. Meeting, Am.Soc. Photogramm., Deyton, Ohio.

LEWIS A.J. and H.C. MACDONALD (1970): "Interpretive and Mosaicking Problems of SLAR Imagery". Remote Sensing of Environment, Vol. 1, No. 4.

LING C., L. RASMUSSEN, W. CAMPBELL (1978): "Flight Path Curvature Distortion in Side-Looking Airborne Radar Imagery". Photogramm. Eng. and Remote Sensing, Vol. 44, No. 10.

LOELKES G.L. (1965): "Radar Mapping Imagery-Its Enhancements and Extraction for Map Construction". Pres. Paper, Fall Tech. Meeting, Am. Soc. Photogramm., Dayton, Ohio.

LOSHCHILOV, U.S., U.A. VOYEVODIN (1972): "Determining Elements of Drift of the Ice Cover and Movement of the Ice-Edge by the Aid of the TOROS Aircraft Lateral Scan Radar Station". Problemi Ariki, Antartiki, No. 40, Moskow.

LUCHININOV V.S. (1975): "Contactless Radar Mapping of Warm Valley Glaciers-Transformation of Radar Coordinates". Transl. from Russian in Soviet Physics-Technical Physics, Vol. 20, No. 4, 1976.

MACCHIA R.P. (1957): "Radar Presentation Restitutor". Photogramm. Eng., Vol. 23.

MANUAL OF PHOTOGRAMMETRY (1966): "Photogrammetric and Radargrammetric Techniques". Vol. II, 3rd Ed.

MARTIN-KAYE P.H. et al. (1980): "Fracture Trace Expression and Analysis in Radar Imagery of Rain Forest Terrain (Peru)". In Radar Geology. An Assessment, JPL-Publication 80 - 61, Jet Propulsion Lab., Pasadena, USA.

MASRY S.E., E.E. DERENYI, B.G. CRAWLEY (1976): "Photomaps from Non-Conventional Imagery". Photogramm. Eng. and Remote Sensing, Vol. 42, No. 4.

MATHEWS R.E. (1975): "Active Microwave Workshop Report". NASA Special Report SP-376, Washington, C.D.

MC KEOWN J.B. (1979): "Remote Sensing of the Resources of Los Andes Region". Venezuela, Final Report, - Vol. I. Environmental Research Institute of Michigan, Report 305 200-7-F, Ann Arbor, Michigan.

MOORE R.K. (1969): "Heights from Simultaneous Radar and Infrared". Photogramm. Eng., Vol. 35.

MOREIRA H.F. (1973): "Project RADAM-Remote Sensing Application to Environmental Analysis of Amazon Region". 2nd Annual Remote Sensing of Earth Resources Conference, Univ. of Tennessee Space Inst., Tullahoma, Tennessee.

MUHLEMAN (1964): "Radar Scattering from Venus and the Moon", Astronomical Journal, Vol. 69, p. 34

NARAGHI M., W. STROMBERG, M. DAILY (1981): "Geometric Rectification of Radar Imagery Using Digital Elevation Models". Image Processing Laboratory of the Jet Propulsion Laboratory, Pasadena, USA.

NORVELLE R.R. (1972): "As-11-A Radar Program". Photogramm. Eng., Vol. 38.

OSWALD H., H. RAETZSCH (1984): "A System for Generation and Display of Digital Elevation Models". Geo-Processing, Geo-Data, Geo-Systems and Digital Mapping; Elsevier Scientific Publishing Company, 1000 AH Amsterdam, Netherlands.

PETERSON R.K. (1976): "Radar Correlator Geometric Control". Goodyear Aerospace Report GIB 9397, Litchfield Park, Arizona; Pres. Paper, 13th Cong. Int. Soc. Photogramm., Helsinki, Finland.

PHILLIPS R.J. et al.(1973): "Apollo Lunar Sounder Experiment". Apollo 17 Preliminary Science Report, NASA Special Publication SP-330, Washington, D.C.

PROTHERSE W.M. et al. (1950): "The Geometry of the Radarscope". Techn. Paper, No. 107, Mapping and Charting Laboratory Ohio State Univ., Ohio.

RADAR GEOLOGY (1980): "Radar Geology". An Assessment, JPL Publication 80 -61, Jet Propulsion Lab., Pasadena, USA.

RAGGAM J. (1985): "Untersuchungen und Entwicklungen zur Stereo-Radargrammetrie". DIBAG-Report, Graz Research Center, 152 p.

RANEY K. (1981): "Radarsat Programme". Presented Paper, ISPRS-SAR Processing Working Group II 15, Frascati, Italy, 3 - 4 Dec.

RAYTHEON CO. (1973): "Digital Rectification of Side-Looking Radar (DRESLAR)". Final Report, Raytheon Co., Autometric Operation, Proep. for US Army Engineer Topographic Laboratories, Fort Belvoir, Virginia 22060, Report No. ETL-CR-73-18.

RINNER K. (1948): "Die Geometrie des Funkbildes". Austrian Academy of Sciences, Math. Naturwiss. Klasse, also in "Handbuch der Vermessungskunde", Jordan-Eggert-Kneissl, Vol. VI, Metzlersche Verlagsbuchhandlung, Stuttgart.

ROESSL J. VAN and R. DE GODOY (1974): "SLAR Mosaics for Project RADAM". Photogramm. Eng., Vol. 40.

ROSENFIELD G.H. (1968): "Stereo Radar Techniques". Photogramm. Eng., Vol. 34.

RYDSTROM H.C. (1968): "Radargrammetric Applications of the Right Angle Solution Nomogram". Goodyear Aerospace Corp., Report GIB 9124, Litchfield Park, Arizona.

SCHEPS B.B. (1960): "To Measure is to Know-Geometric Fidelity and Interpretation in Radar Mapping". Photogramm. Eng., Vol. 36.

SCHERTLER R.J. et al. (1975): "Great Lakes All-Weather Ice Information System". Proc, 10th Symp. Remote Sensing of the Environment". Ann Arbor, Michigan.

SCHREITER J.B.(1950): "Strip Projection for Radar Charting". Techn. Paper No. 130, Mapping and Charting Lab., Ohio State Univ., Ohio.

SCHWARZ H.R. (1970): "Die Methode der konjugierten Gradienten in der Ausgleichsrechnung". Zeitschrift f. Vermessungswesen, Vol. 1970, 4.

SHAKINE A., T. LE TOAN (1978): "A Study of Digitized Radar Images". Intl. Symp. of Remote Sensing of Environment, Ann Arbor, USA.

SMITH H.P. (1948): "Mapping by Radar - The Procedures and Possibilities of a New and Revolutionary Method Mapping and Charting". U.S. Air Force, Randolph Field, Texas.

STILWELL J.E. (1963): "Radar Network Adjustment". Photogramm. Eng., Vol. 21.

SUPER A.D. et al. (1975): "Remote Sensing Applied to the International Ice patrol". Proc. 10th Symp. on Remote Sensing of the Environment, Ann Arbor.

TELEKI P., R. RAMSEIER (1978): "The Seasat-A Synthtic Aperture Radar Experiment". Proc. Intl. Symp. Comm. VII of Intl. Soc. of Photogrammetry, July 2 - 8, Univ. of Freiburg, Vol. 1.

TIERNAN M. et al. (1976): "Lunar Cartography with the Apollo 17 Radar Imagery". The Moon, Vol. 15, No. 1/2.

THOMAN G. (1969): "Distance Computation on Radar Film". Simonnett, D.G. (ed.), "The Utility of Radar and Other Remote Sensors in Thematic Land Use Mapping from Spacecraft", Annual Report, NASA-140.

THOMPSON T.W. et al. (1972): "Progress Report on 25 cm Radar Observations of the 1971 AIDJEX Studies". Arctic Ice Dynamics Joint Experiment (AIDJEX) Bulletin, No. 12, Univ. of Wash., Seattle Wash.

ULABY F.T., C. DOBSON, I. STILES, R.K. MOORE, I. HOLTZMAN (1982): "A Simulation study of Soil Moisture Estimation by a Space SAR". Photogramm. Eng. and Remote Sensing, Vol. 48, No. 4.

YORITOMO K. (1965): "All Waether Mapping". Presented Paper, Fall Technical Meeting, Soc. Photogramm., Deyton, Ohio.

YORITOMO K. (1972): "Methods and Instruments for the Restitution of Radar Pictures". Arch.Int. Soc. Photogramm., Invited Paper, 12th Congress, Ottawa, Canada.

ZHURKIN I.G., N.KORNEYEV (1974): "Relationship between the Coordinates of Terrain Points and the Coordinates of Image Points in Side-Looking Radar Systems with an Antenna along the Fuselage". Geodesy, Mapping, Photogrammetry, Vol. 16, No. 3.